An Acad Bras Cienc (2023) 95(Suppl. 3): e20230722 DOI 10.1590/0001-3765202320230722
Anais da Academia Brasileira de Ciências | *Annals of the Brazilian Academy of Sciences*
Printed ISSN 0001-3765 I Online ISSN 1678-2690
www.scielo.br/aabc | www.fb.com/aabcjournal

SOIL SCIENCE

Ornithogenesis and soil-landscape interplays at northern Harmony Point, Nelson Island, Maritime Antarctica

IORRANA F. SACRAMENTO, CARLOS ERNESTO G.R. SCHAEFER, RAFAEL G. SIQUEIRA, GUILHERME R. CORRÊA, JAIR PUTZKE, ROBERTO F.M. MICHEL & MÁRCIO R. FRANCELINO

Abstract: Understanding the influence of soil-forming factors and processes in ornithogenic soils is important to predict impacts of climate change on Antarctic ecosystems. Herein, we analyzed the soil-landscape interplays and development of ornithogenic soils at Harmony Point (HP), Nelson Island. We collected, described, and classified 24 soil profiles, combined with vegetation and landforms descriptions. Geoprocessing techniques were employed for mapping. Soil physical, chemical, geochemical, and mineralogical analyses were applied. Patterned ground, "Ornithogenic"/ Typic Gelorthent, and moss carpets were the dominant landform, soil and vegetation classes, respectively. Soils from rocky outcrops were more structured, acidic, with higher organic carbon, organometallic complexes, and secondary phosphate minerals, due to former bird influence. Soils from cryoplanated platforms presented higher water pH, base saturation, clay content, and secondary silicate minerals. Soils from marine terraces presented high exchangeable bases, phosphorous, and amorphous phosphate minerals. Soil chemical weathering is enhanced by ornithogenesis and widespread in HP. Besides ornithogenesis, organic matter accumulation, cryoturbation, and cryoclastic processes are also important to pedogenesis of ornithogenic soils. The soils of the cryoplanated platforms exhibited a gradient of pedogenetic development corresponding to increasing biota influence and distance from glacier. In contrast, soils of rocky outcrops were more developed even close to the glacier, due to ornithogenesis.

Key words: cryosols, cryoturbation, pedogenesis, phosphatization.

INTRODUCTION

In general, Antarctic soils are poorly developed due to the cold and dry climate (Campbell & Claridge 1987), with physical, chemical, and morphological properties strongly related to the parent material (Simas et al. 2008). Seabird influence is one of the main factors driving chemical weathering and pedogenesis on the continent (Balks et al. 2013), leading to the formation of some of the Antarctica's most developed soils, known as ornithogenic soils (Simas et al. 2007). Ornithogenesis is more evident in the wetter and warmer maritime Antarctic (MA) region, where ornithogenic soils are widespread in active or abandoned bird colonies along the coastal zone (Tatur & Myrcha 1984, Tatur 1989). Ornithogenesis also extends indirectly to areas adjacent to colonies through subsurface and surface lateral flow, which helps to magnify bird impacts (Tatur 2002). Although ornithogenesis is best expressed under the influence of penguins due to the larger population size (Simas et al. 2007), flying birds are also capable of influencing soil formation near their nesting sites (Abakumov et al. 2021a, b, Lopes et al. 2022, Rodrigues et al. 2021b).

Ornithogenic soils are influenced by the deposition and microbial decomposition of P-rich guano, whose leachate interacts with the mineral substrate to produce intense geochemical and mineralogical changes through the phosphatization process (Rodrigues et al. 2021a, b, Simas et al. 2007, Tatur & Myrcha 1984). One of these changes is the progressive acidification of the soil as result of secondary processes such as nitrification (Myrcha et al. 1985). Phosphatization is also responsible for the dissolution of primary aluminosilicates and the formation of non-crystalline and crystalline phosphates precipitated from reactions between P leachates and weathering products (Haus et al. 2016, Tatur & Barczuk 1985, Tatur & Keck 1990). The newly formed phosphates, in turn, affect many morphological and physicochemical properties of soils such as color, texture, structure and surface charge.

From a biogeochemical perspective, Antarctic ornithogenic soils act as a temporary reservoir of nutrients. During the breeding season, seabirds transfer large amounts of nutrients from the sea to the land by depositing excreta rich in C, P, N and trace metals such as Cu, Zn, Cr and Hg (Castro et al. 2021, 2022, Tatur & Myrcha 1984). Seabird populations in Antarctica and the Southern Ocean account for 80% of the total N and P excreted by seabirds worldwide (470 and 79 Gg y^{-1}, respectively) (Otero et al. 2018). Some C and N is volatilized by bacterial mineralization (Pietr et al. 1983), releasing ammonia and greenhouse gases (Ferrari et al. 2022); (Zhu et al. 2009, 2011). Most of the nutrients are removed by drainage, lateral leakage, or wind erosion and can re-enter the ocean through eutrophication of coastal waters. The higher annual losses are associated primarily with N, although in soils with permafrost, P losses can increase substantially due to rapid soil P saturation (Otero et al. 2018). In turn, phosphatization is activated only by the smallest fraction of P that remains in the soil, which can be more than 10% under favorable conditions (Pereira et al. 2013).

Ornithogenesis is the predominant factor in increasing soil carbon stocks in MA, especially in abandoned sites where the dense vegetation cover favors the accumulation of organic matter and the formation of deep organic horizons (Tatur 1989, Tatur et al. 1997). The organic matter in these soils consists mainly of readily degradable compounds (Michel et al. 2006), making them a potential source of CO_2 prior to climate change scenarios (Convey & Peck 2019). Ornithogenesis also models vegetative biodiversity by creating favorable microenvironments for plant colonization and diversification (Ferrari et al. 2021, Schmitz et al. 2020a) and favors specialized soil microorganisms adapted to the unique chemical properties of ornithogenic soils (Ramírez-Fernández et al. 2019).

In addition to the influence of birds, other factors play an important role in pedogenesis in MA, such as parent material (Moura et al. 2014, Navas et al. 2008), geomorphic processes (Francelino et al. 2011, González-Guzmán et al. 2017), and vegetation (Otero et al. 2013, Poelking et al. 2015). However, few studies have focused on how the interactions of these soil-forming factors directly influence the development of ornithogenic soils. Previous studies in the southern sector of Harmony Point (HP) have shown that the ornithogenic influence is extensive and increased chemical weathering and soil development (Rodrigues et al. 2019). Here, our main objective was to examine the soil-landscape interactions, particularly in relation to relief, parent material and vegetation, and how they influence the development of ornithogenic soils at the northern sector of HP, Nelson Island. For this purpose, we combined a set of spatial, physical, chemical, geochemical, and mineralogical data to understand the effects of the soil forming factors and identify the pedogenetic processes interacting with the phosphatization to form the ornithogenic soils of HP.

MATERIALS AND METHODS

Study area

Nelson Island is in the South Shetland Islands (SSI), one of the archipelagos of the MA, and presents a total area of 165 km², with only 5% of the area ice-free. HP is located at the northwestern part of Nelson Island (59°12'46.68" W and 62°17'36.456" S), with an area of 4 km² (Figure 1). According to the Bellingshausen meteorological station, located at Fildes Peninsula (15 km of distance) in King George Island, in the last 54 years the mean annual temperature of the region was -2.25 °C and the mean summer temperature was 1.12 °C (BAS 2020). The mean annual precipitation in Bellingshausen is around 817 mm, with rainy summers and the climate of the SSI is defined as mild, maritime climate (Turner & Pendlebury 2004).

The geology of HP is mainly characterized by Paleocene-Eocene basaltic andesites, pyroclastic rocks, as breccias and lapillistones, and microgabbro intrusions (Smellie et al. 1984). As the others ice-free areas of SSI, HP presents raised marine terraces as the result of the glacio-isostatic uplift after the Late Glacial Maximum (LGM) during Holocene, approximately 9 ka BP (Hjort et al. 1998, John & Sugden 1971). The LGM is also evidenced in the area by the presence of drifts, striated rocks, and erratic blocks. The upper platforms are marked by the presence of large patterned ground fields (Rodrigues et al.

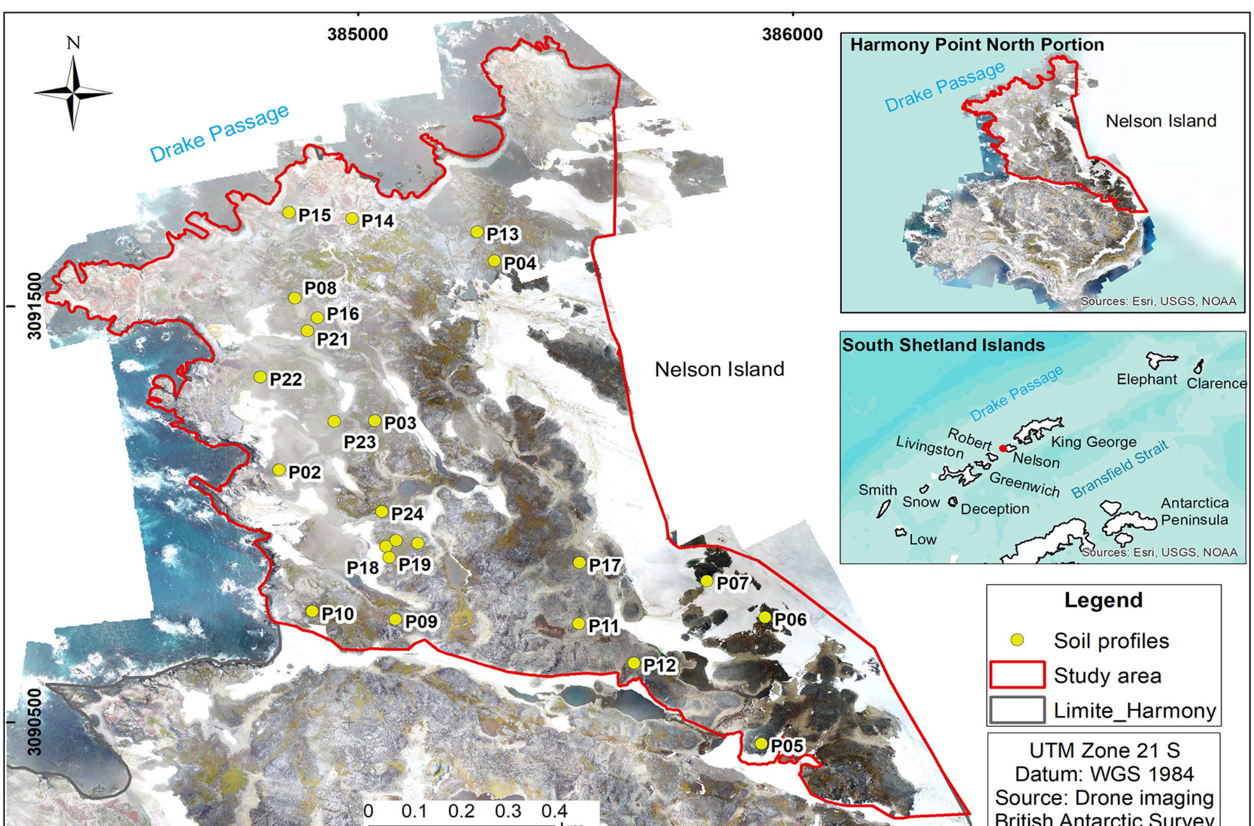

Figure 1. Location map of the study area: northern sector of Harmony Point, Nelson Island, Maritime Antarctica.

2019), evidencing the stability of the periglacial landscape.

Due to its biological diversity and ecological significance, HP is an Antarctic Specially Protected Area (ASPA 133). HP presents breeding colonies of 12 bird's species, such as chinstrap penguins (*Pygoscelis antarctica*), gentoo penguins (*Pygoscelis papua*), giant petrels (*Macronectes gianteus*), kelp gulls (*Larus dominicanus*), brown skuas (*Catharacta antarctica*) and south polar skuas (*Catharacta maccormicki*). There are also mammal species like the Weddell seals (*Leptonychotes weddelli*), the Antarctic fur seals (*Arctocephalus gazella*) and the southern elephant seal (*Mirounga leonina*) (ATCM XXXV 2012). The vegetation of HP is very abundant and diverse, presenting many species of wide mosses usually associated with lichens or macroalgae, mainly in the protected and moister sites, whereas crustose lichens predominate in the exposed dryer areas.

Fieldwork and mappings

Soil sampling occurred during the 2019 summer season, from January to February. We collected samples of 24 soil profiles and described their morphological features. The soils were classified according to the Soil Taxonomy (SSS 2014) and the World Reference Base for Soil Resources (IUSS Working Group WRB 2014) systems. Landforms were identified according to previous geomorphological studies in MA (Francelino et al. 2011, López-Martínez et al. 2012, Michel et al. 2014, Oliva & Ruiz-Fernández 2017, Rodrigues et al. 2019, Pallàs et al. 1995). The vegetation description was performed in the field around each soil profile described, referring to specialized classification guides for MA (Ochyra et al. 2008, Olech 2004, Putzke & Pereira 2001).

We conducted an aerial imaging over the study area using a remotely piloted aircraft (RPA) DJI Phantom 4. The images were processed using the Agisoft® Metashape software and an orthomosaic of the aerial images with approximately 0.05 m spatial resolution was generated. Soil and geomorphological maps were generated by photointerpretation over the orthomosaic. We considered the Soil Taxonomy classes for the soil mapping. The vegetation map was obtained with the image's visible bands and the Green-Red Vegetation Index (GRVI) (Tucker 1978), besides applying a semi-automated classification, associating object-oriented techniques (segmentation) followed by labelling the segments by visual interpretation. The vegetation classes were adapted from the subformation classes proposed by Longton (1988), which were based on growth form of the community dominants. The final 1:10.000 maps were created using the ESRI® ArcGIS software tools.

Physical, chemical, and mineralogical soil analyses

Soil samples were air dried and sieved using a 2 mm sieve. Physical and chemical analysis were performed following procedures recommended by the Brazilian Agricultural Research Corporation - EMBRAPA (Teixeira et al. 2017). Soil fractions were extracted by mechanical dispersion of soil samples in distilled water, sieving and weighting of the coarse sand (0.2 – 2 mm) and fine sand (0.05 – 0.2 mm), and sedimentation of the silt fraction (0.002 – 0.05 mm) followed by siphoning of clay (< 0.002 mm).

Soil pH was determined in H_2O and KCl 1 mol L^{-1} in a relation soil-liquid of 1:2.5. Available P, K, Na, Cu, Mn, Fe and Zn were extracted using Mehlich-1 (HCl 0.05 mol L^{-1} and H_2SO_4 0.0125 mol L^{-1}), and determined by photocolorimetry (P), flame emission (K and Na) and atomic absorption spectroscopy (micronutrients). Available S were extracted by a $Ca(H_2PO_5)_2$ solution in acetic acid 2 mol L^{-1} and determined by photocolorimetry. Exchangeable Ca^{2+}, Mg^{2+} and Al^{3+} ions were extracted by KCl 1 mol L^{-1} solution and determined by atomic absorption spectroscopy (Ca^{2+}, Mg^{2+}) and titration (Al^{3+}). The potential acidity (H+Al) was obtained by $Ca(CH_3COO_2)$ 0.5 mol L^{-1} solution buffered at pH 7 and titration. The capacity of soil to adsorb P (P-rem) were obtained by a $CaCl_2$ 0.01 mol L^{-1} solution and measured by photocolorimetry. From those elements we calculated the base sum (BS = Ca^{2+} + Mg^{2+} + K^+ + Na^+), effective cation exchange capacity (eCEC = BS + Al^{3+}), potential cation exchange capacity (pCEC = BS + H + Al), percentage of base sum (PBS = BS/pCEC * 100), aluminum saturarion (Al_{sat} = Al^{3+}/eCEC*100) and sodium saturation (NaSI = Na/eCEC*100).

Total Organic Carbon (TOC) and total Nitrogen (TN) were obtained by wet combustion methods (Yeomans & Bremner 1988, Kjeldahl 1883), respectively. Total P (TP) were obtained by a sequential extraction of concentrated H_2SO_4, H_2O_2 40% and concentrated HF (Bowman 1989) and determined by inductively coupled plasma optical emission spectrometry (ICP-OES). We also quantified different fractions of pedogenic Fe and Al: total pedogenic Fe and Al (Fe_d and Al_d) extracted by Dithionite-Citrate-Bicarbonate (DCB) (Mehra & Jackson 1960), Fe and Al associated to non-crystalline forms (Fe_o and Al_o) extracted by Ammonium Oxalate (McKeague & Day 1966) and Fe and Al forms bounded to soil organic matter (Fe_p and Al_p) extracted with sodium pyrophosphate at pH 10 (Dahlgren 1994). The extractions content was determined by atomic absorption spectroscopy.

Contents of Al, Ca, Fe, K, Mg, Na, Si, Ti, P, S, Zn, Cu, Co and Mn were obtained by a semi-quantitative analysis using the micro energy dispersive X-Ray fluorescence (µ-XRF – 1300 Shimadzu). Samples were passed through a 200-mesh sieve and pressed with a hydraulic press to produce 2 mm soil pellets. The µ- XRF, equipped with a X-ray tube and a Si detector, was calibrated using the certified reference material Soil Montana II (SRM 2711a). Mineralogical analysis was performed over oriented clay samples and non-oriented silt and sand samples using X-ray diffraction (XRD), with the PANalytical/X'PertPro Diffractometer, of CoKα radiation in a 4 – 50° 2θ range. In addition, clay samples were treated with $MgCl_2$ 0.5 mol L^{-1}, 10% glycerol solvation and KCl 1 mol L^{-1} saturation at 25, 350 and 550 °C.

Statistical analysis

The soils were divided into three groups according to the representative landscape units of the north of HP: i) soils of the rocky outcrops (SRO); ii) soils of the platforms (SP); and iii) and soils of the marine terraces (SMT). Using the stats and rstatix packages in the software R, we performed the non-parametric Kruskal-Walliss and the post-hoc Dunn's tests to compare the significance of the differences between these soil groups. We also applied a Principal Component Analysis (PCA), using the FactoMineR package, to identify similarity patterns between physical and chemical data of selected soil samples. Finally, we use the Spearman's rank correlation coefficient to identify the strength of the associations between some chemical soil attributes. The significance of these results was estimated considering a 95% confidence interval (p value ≤ 0.05) from Student's t test.

RESULTS

Environmental features and mapping

Geomorphology

Three main landscape units were observed at the northern sector of HP: (i) the coastal area, (ii) the periglacial area, (iii) and the paraglacial area, considering the main landforms and associated processes. A talus slope marks the transition between the coastal and the higher (periglacial and paraglacial) areas and is strongly dissected by drainage channels and nivation niches. In the higher areas, the landscape follows a gradient of soil development related to the time of exposure to non-glacial processes.

The coastal landforms cover 26% (39 ha) of the total mapped area (150 ha) (Figure 2). The coastal environment is composed of beaches, marine terraces, rocky cliffs and volcanic stacks (Figure 3a). The Drake passage coastline has very jagged edges, due to the stormy erosive action of the gales and waves, which lead to the formation of narrow, poorly developed beaches and very eroded rocky cliffs and volcanic stacks, which are widely colonized by penguins (Figure 3b). The marine terraces are cut off by drainage channels and present many rock fragments from the volcanic stacks' erosion. They are the result of the glacio-isostatic uplift occurred in the SSI during the Holocene (John & Sugden 1971). In HP, there are three different levels of marine terraces (first level ranges from 2 – 5 m, the second one from 5 – 7 and the third one from 7 – 10 m above sea level), limited by sand ridges representing each uplift pulse (Figure 3c).

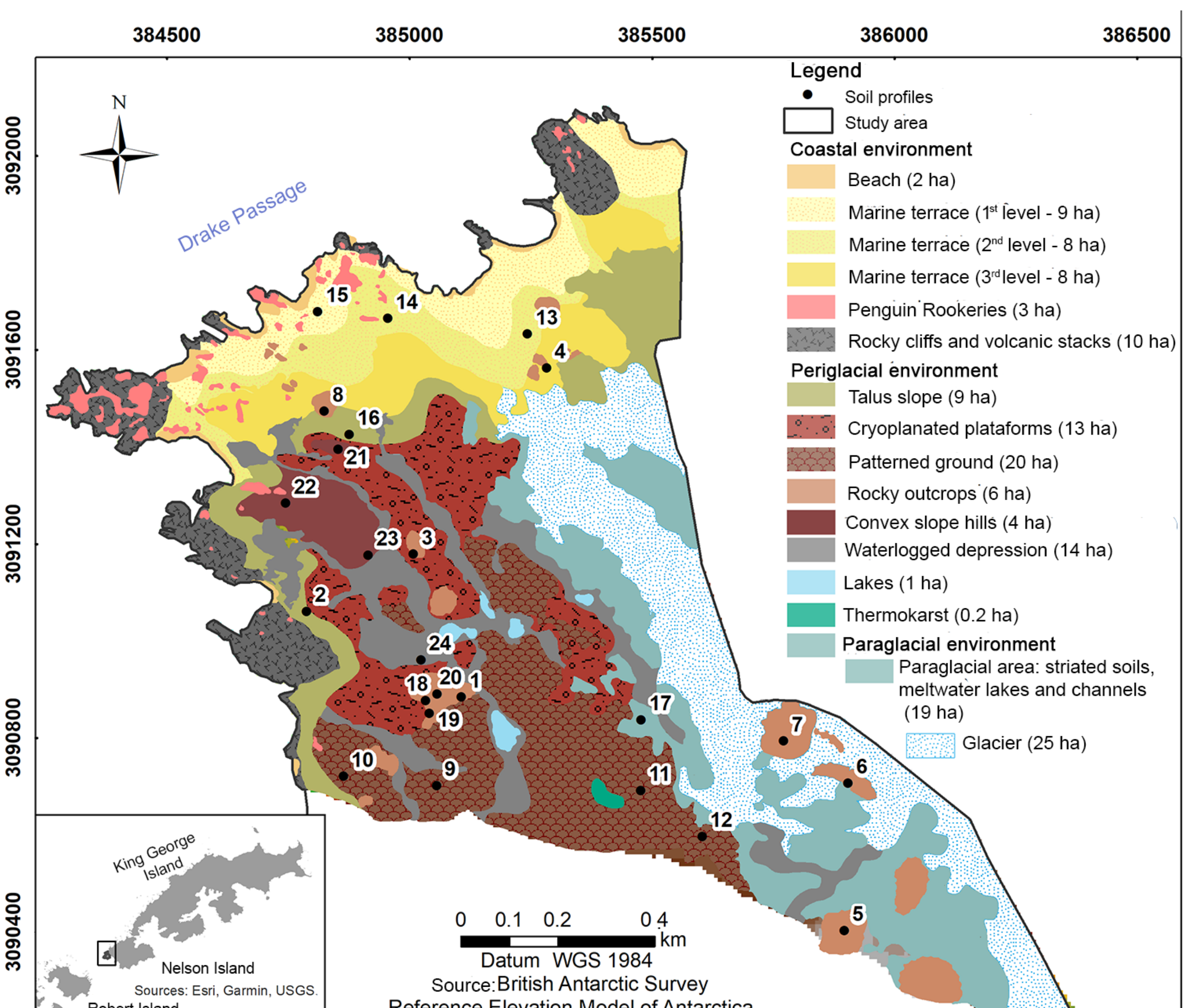

Figure 2. Geomorphological map of the northern sector of Harmony Point.

The transition zone from the coastal environment of the marine terraces to the periglacial areas is irregular, with steep or gentle convex slopes dissected by drainage channels and depressions where snow accumulates. Along the transition zone there are numerous rocky outcrops corresponding to ancient volcanic plugs, formerly occupied by penguins and petrels nests, which still occur sporadically. In general, the northern side of such outcrops, facing the Drake sea, is more eroded than the southern side, due to the influence of strong winds from the Drake Passage.

The periglacial environment of HP is composed by flat to wavy cryoplanated platforms, patterned ground, rocky outcrops, convex slopes hill, waterlogged depressions, talus slopes, thermokarsts and lakes. The periglacial landforms cover 45% (67 ha) of the mapped area, being the predominant landscape unit of the northern sector of HP (Figure 2). We observed two levels of platforms (Figure 3d) in HP, corroborating to Rodrigues et al. (2019), being the upper platform located approximately at 35 - 45 m and the lower one from 25 - 35 m a.s.l. The origin of these platforms in the SSI is related to marine erosion along successive fluctuations of the sea-level during the last interglacial period (Barsch & Mäusbacher 1986, John & Sugden 1971). These platforms correspond to ancient drifts formed due to the glacier overrunning during the LGM, as evidenced by striated pavements,

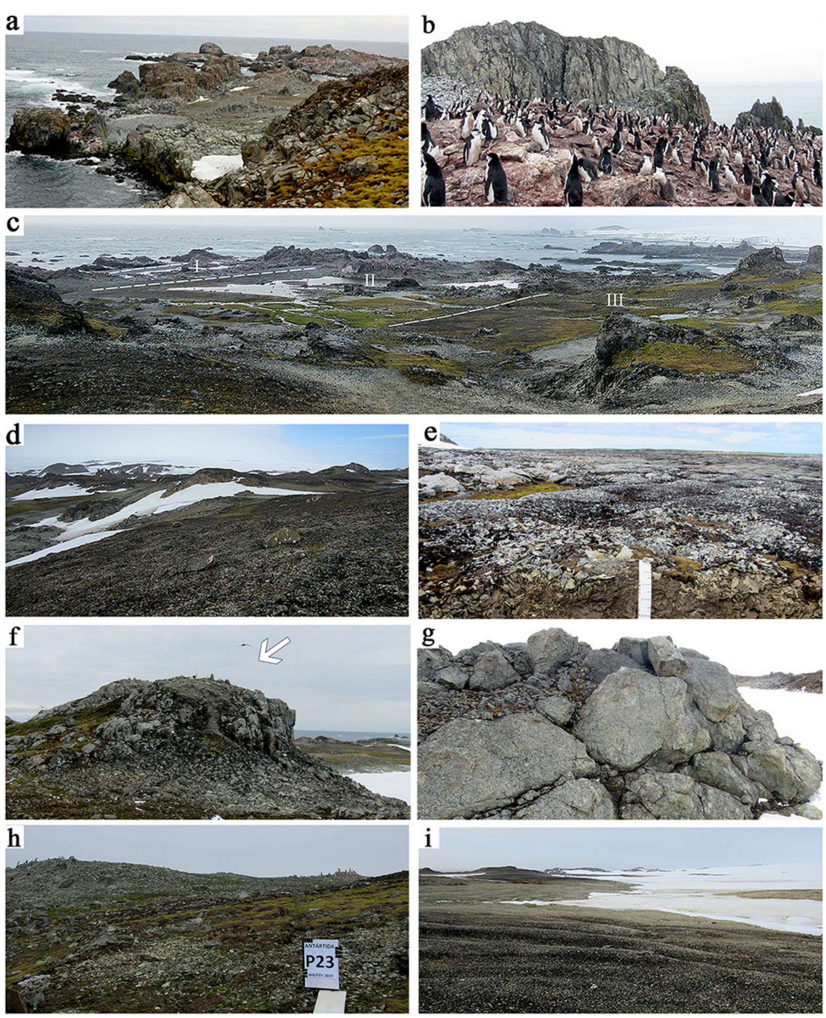

Figure 3. **Main landforms of the northern sector of Harmony Point. a) Rocky cliffs and volcanic stacks; b) Rocky cliffs with penguin rookeries; c) Three uplifted marine terrace levels; d) Talus slopes in the transition between the coastal and the paraglacial environments; e) Patterned ground on the high platform; f) Rocky outcrops with giant petrels' nest; g) Rocky outcrops with pre-weathered material, releasing rounded corestones; h) Convex slope hills with present ornithogenic influence; i) Striated patterned ground in the paraglacial area.**

and degraded “Roche moutonnée” (Rodrigues et al. 2019). After a long time of exposure, periglacial processes have been active in these platforms, with mainly permafrost and cryonival related processes.

The patterned ground represents the maximum level of periglacialism at HP, indicating a long time of exposure and the occurrence of processes associated to the freeze-thaw soil processes, such as frost heaving and sorting. They predominate over the upper platform, occupying 13% (20 ha) of the total area. In the northern sector of HP, soils with circular patterns predominate in flat areas, and transitional forms (labyrinthine to elongated) tending to striated occur in slightly sloping areas where gelifluction is more active (Figure 3e).

The rocky outcrops occur predominantly as residuals on the platforms and represent 6.6% (10 ha) of the total area (Figure 3f). This landform is composed by plugs of andesitic basalts, which are very resistant to weathering, in comparison of the other rocks presented in the area. The rocky outcrops of HP can be characterized as “roche mountonée” (Rodrigues et al. 2019). It is common to find rocky outcrops with preserved crests, which are largely occupied by giant petrels nests. In the surrounding areas of the rocky outcrops debris accumulates, presenting large and angular rock fragments that occurs *in situ*. Some outcrops present rounded blocks in subsurface (corestones), resulting from the action of paleoweathering on the edges of rock fragments (Figure 3g). In the interior of the platforms there are hills with convex slopes (Figure 3h) developed from ancient rocky outcrops. These landforms are more developed, due to the longer exposure to weathering processes such as eolian, pluvial, and gravitational processes, but mostly periglacial ones (cryoturbation, nivation, frost creep), which favor the formation of a smooth wavy relief. Currently, the chemical weathering of the rocky outcrops is intensified by the phosphatization process due to guano deposition in closed fractures and microdepressions, as observed in other SSI areas (Lopes et al. 2022).

The paraglacial areas represent a more unstable landscape, transitioning from glacial to non-glacial conditions (Ballantyne 2013, Slaymaker 2011). They are younger than the periglacial areas and non-glacial processes, such as fluvial, lacustrine, gravitational and aeolian, predominate. The paraglacial areas of the northern sector of HP encompasses 13% (19 ha) of the mapped area and are located closer to the glacier (Figure 2). These areas are characterized by the presence of proglacial lakes and a drainage system of meltwater, responsible for sediment transport to the low coastal areas. Less developed periglacial landforms can be found in gently sloping areas, in the transition to the periglacial areas, such as non-sorted steps, forming a striated pattern on the ground (Figure 3i).

The waterlogged depressions and lakes encompass 9.9% (15 ha) of the total area. They are formed by drainage incisions of glacial waters, mainly in the depressions closer to the glacier, and by snow melting during summer, forming seasonal water regime channels (Francelino et al. 2011). The origin of the waterlogged depressions and lakes are also related to solifluction and permafrost degradation, which is evidenced by the occurrence of thermokarsts. These features correspond to shallow depressions common in areas of attenuation and inactivity of thaw-freeze processes (López-Martínez et al. 2012).

Soil classes

The soil classes mapping comprises 69% (104 ha) of the total area, excepting those where soil development was absent, such as glacier, beaches, volcanic stacks, some paraglacial areas and water bodies (Figure 4). The “Ornithogenic”/Typic Gelorthent mapping unit is the most representative in the northern sector of HP (Figure 5a), covering 13% (19 ha) of the total area, and predominates in the rocky outcrops and hills of the platforms, and in the third level of the marine terraces. The Typic Aquiturbel was the second largest unit, covering 8.7% (13 ha) of the total area, and predominates in the patterned ground area. The Typic Gelaquent unit covers 7.3% (11 ha) of the total area and prevails in the waterlogged depressions.

The Entisol (Regosol and Leptosol on WRB/FAO) was the most frequent soil order in HP, covering 36% (54 ha) of the total area (Figure 4) and it occurs in most landforms, as marine terraces, talus slope, flat platforms, rocky outcrops, hills, and waterlogged depressions (Table I). This soil order represents the soils with the least pedogenetic development in HP, due to the parent material resistance to weathering, water saturation and sand content. The Entisols are distributed according to areas where permafrost is sporadic or absent, such as the coastal areas with < 25 m of altitude, and discontinuous, as the surfaces of 25 – 80 m (Balks et al. 2013, López-Martínez et al. 2012, Bockheim et al. 2015). The Gelorthent suborder was found on the rocky outcrops, due to the lithic contact within 20 cm soil depth. The Gelaquent suborder was mainly in the marine terraces and waterlogged depressions areas where the water table is closer to the surface. The Cryopsamment suborder was identified in the second level

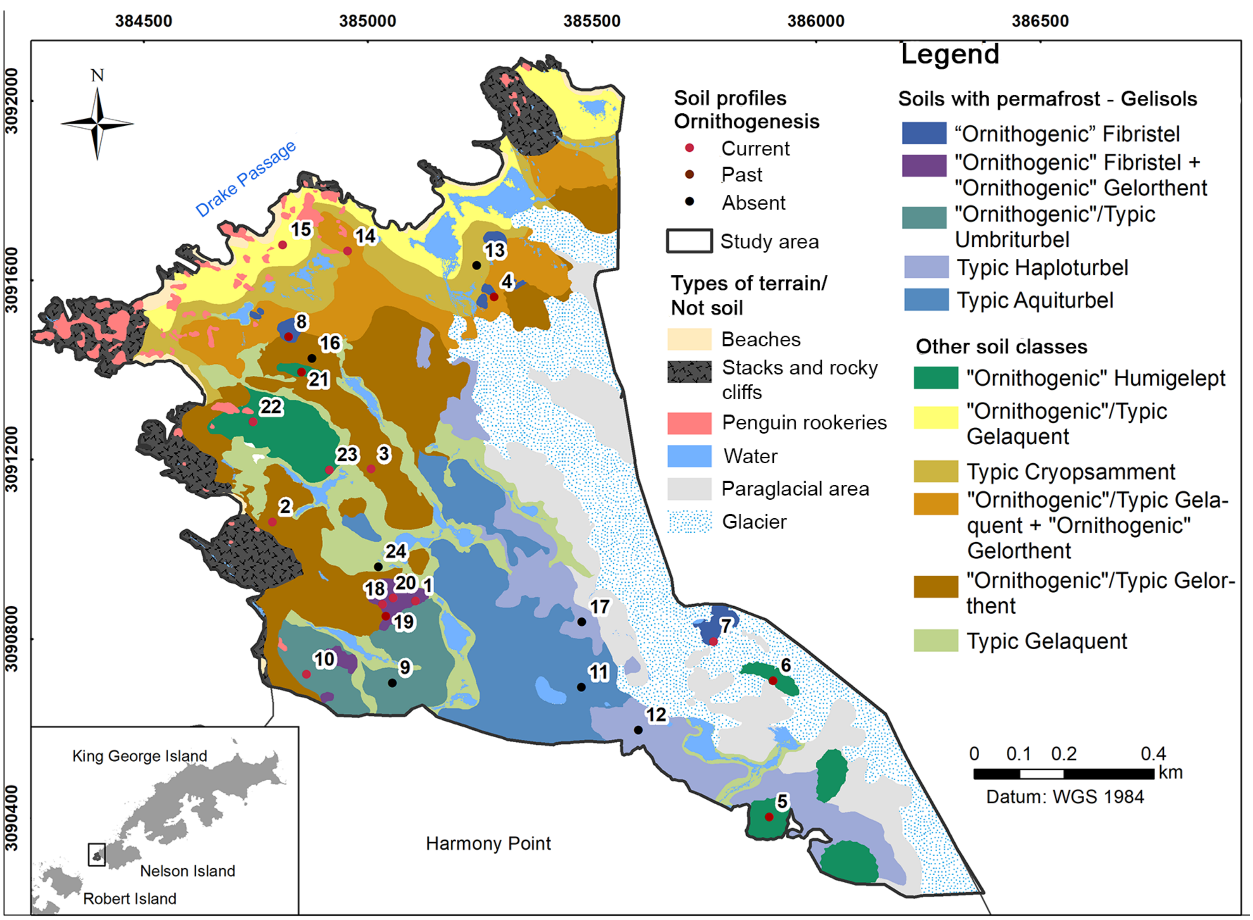

Figure 4. Soil class map of the northern sector of Harmony Point, Nelson Island, Maritime Antarctica.

marine terrace, due to the typical sandy texture of marine depositional environments.

The Gelisols (Cryosols on WRB/FAO) cover 20% (29.5 ha) of the total area (Figure 4) and are characterized by presenting permafrost within the first 100 cm soil depth, or gelic materials (cryoturbation) within the first 100 cm and permafrost in 200 cm from soil surface (SSS 1999). In HP, they occur between 22 – 56 m of altitude, in the rocky outcrops and patterned ground, and in some paraglacial areas. The Histel suborder are represented by the Fibristel great group (Folic Cryosols on WRB/FAO), which are soils that have more fibric materials than other kind of organic material. The Turbel suborder (Turbic Cryosols on WRB/FAO) presented cryoturbation evidence such as cryoturbated soils (patterned ground), irregular and/or broken horizons, organic matter accumulation on top of permafrost table, oriented rock fragments, frost heaving and solifluction (Bockheim & Tarnocai 1998). The great groups were Aquiturbels (present aquic conditions and redox depletions, Figure 5c), Umbriturbels (Umbric epipedon) and Haploturbels.

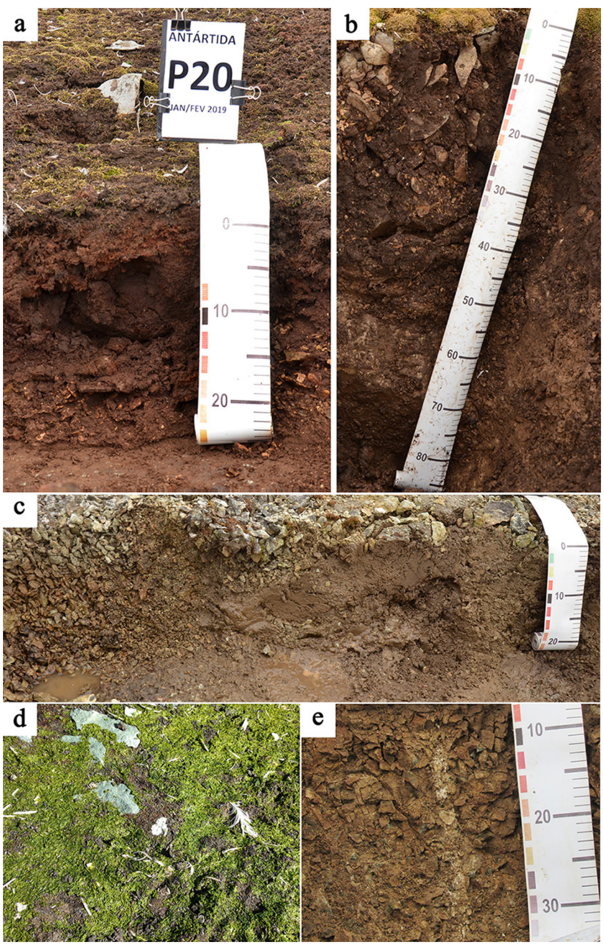

Figure 5. Most representative soil classes and morphological features indicating the ornithogenic influence in the soils of the northern sector of Harmony Point. a) "Ornithogenic" Gelorthent (P20) in a rocky outcrop; b) "Ornithogenic" Humigelept (P5) at a rocky outcrop; c) Typic Aquiturbel (P12) in a patterned ground area; d) Feathers, whitish gravel surfaces and Prasiola crispa vegetation cover; e) Phosphatic vein within the P22 soil profile.

The Inceptisols (Cambisols on WRB/FAO) cover only 4% (6 ha) of the total area (Figure 4) and they occur mainly in the rocky outcrops' debris slopes and in convex slopes hill (Figure 5b). This soil order represents soils with a cambic horizon within the first 100 cm soil depth, with a minimum thickness of 15 cm (SSS 2014). Although in a global pattern they are considered an incipient developed soil, in HP the Inceptsols are the soils with the most pedogenetic development despite of the cold climatic conditions, due to the great time of exposure to weathering processes after the LGM, ornithogenesis and greater vegetation cover. The Inceptisols of the northern sector of HP were identified as Humigelepts (Dystric Skelectic Cambisol on the WRB/FAO), due to the presence of organic and/or umbric horizons.

From the 24 collected soil profiles, 17 presented ornithogenic influence (Table I). The evidence of ornithogenic influence were fresh guano, nesting pebbles, feathers, eggshells, phosphatic veins (accumulation of phosphatic material within the soil profile), whitish horizons or rock surfaces (Figure 5d and 5e). From the 17 ornithogenic soils, seven corresponded to Entisols, five to Gelisols and five to Inceptisols. Most of the ornithogenic soils are in the rocky

Table I. Altitude, landforms, soil classes and ornithogenic influence type.

Profile	Altitude (m)	WRB-FAO Class	Soil Taxonomy Class	Landform	Ornithogenic influence
2	30	Dystric Cambic Folic Leptosol (Ornithic, Turbic)	"Ornithogenic" Gelorthents	Rocky outcrops	Present penguin rookery
3	39	Cambic Lithic Leptosol (Loamic, Ornithic)			Present petrel nest
19	39	Dystric Skeletic Leptosol (Humic, Ornithic)			Abandoned gull nest
20	43	Leptic Folic Regosol (Loamic, Ornithic)			Present petrel nest
22	23	Dystric Skelectic Regosols (Loamic, Humic, Ornithic)			Present penguin rookery
14	6	Dystric Skeletic Regosol (Arenic, Humic, Ornithic)		Second level of marine terrace	Present penguin rookery
16	27	Dystric Skelectic Regosol (Loamic, Humic)	Typic Gelorthent	Talus slope	Non-ornithogenic
4	12	Eutric Stagnic Regosol (Arenic, Humic, Ornithic)	"Ornithogenic" Gelaquents	Third level of marine terrace	Abandoned penguin rookery
15	2	Eutric Skelectic Stagnic Regosol (Arenic, Humic, Ornithic)		First level of marine terrace	Present penguin rookery
24	35	Skeletic Stagnic Regosol (Gelistagnic, Humic)	Typic Gelaquent	Waterlogged depression	Non-ornithogenic
13	6	Eutric Arenosol (Humic)	Typic Cryopsamment	Second level of marine terrace	Non-ornithogenic
1	44	Spodic Folic Leptic Cryosol (Dystric, Ornithic)	"Ornithogenic" Fibristels	Rocky outcrops	Present petrel nest
7	56	Cambic Folic Cryosol (Dystric, Ornithic)			Present petrel nest
8	22				Abandoned penguin rookery
18	39	Histic Leptic Cryosol (Dystric, Ornithic)			Present petrel nest
10-O*	38	Skelectic Turbic Cryosol (Dystric, Humic, Ornithic)	"Ornithogenic" Umbriturbels	Patterned ground	Present penguin rookery
10-B*		Hyperskeletic Turbic Cryosol (Dystric, Ornithic)			
10-C*		Cambic Turbic Cryosol (Dystric, Humic, Ornithic)			
9-O*	37	Hyperskeletic Turbic Cryosol (Dystric, Humic)	Typic Umbriturbels		Non-ornithogenic
9-B*		Hyperskelectic Turbic Cryosol (Dystric, Humic)			
9-C*		Skeletic Turbic Cryosol (Dystric, Humic)			
11-B*	45	Skeletic Turbic Cryosol (Dystric, Humic)	Aquic Haploturbels		Non-ornithogenic
11-C*		Reductaquic Turbic Cryosol (Dystric)	Typic Aquiturbels		
12-B*	37	Hyperskelectic Turbic Cryosol (Eutric, Humic)	Typic Haploturbel		Non-ornithogenic
12-C*		Turbic Cryosol (Eutric, Humic)			
17	40	Hyperskelectic Turbic Cryosol (Dystric, Loamic)		Paraglacial areas near the glacier	Non-ornithogenic
5	59	Dystric Skeletic Cambisol (Humic, Ornithic)	"Ornithogenic" Humigelepts	Rocky outcrops	Present petrel nest
6	61	Folic Leptic Cambisol (Ornithic)			Abandoned gull nest
21	28	Dystric Skeletic Cambisol (Loamic, Ornithic)			Abandoned penguin rookery
23	34	Dystric Skelectic Cambisol (Humic, Ornithic)			Present penguin rookery

*** O corresponds to the outer part of the patterned ground, B represents the border, and C the inner part.**

outcrop slopes, between 22 – 61 m of altitude. In those areas we found present and abandoned nest sites of penguins, kelp gulls and, mostly, petrels. In the upper platform we found one present penguin rookery close to a patterned ground soil profile. Three soils of marine terraces at 2 – 12 m of altitude were under present day penguin rookeries.

Vegetation classes

The cryptogamic vegetation of HP represents 13.3% (19.7 ha) of the total area (Figure 6) and corresponds to the polar tundra, composed mainly by bryophytes, lichens and alga species. The vegetated area predominates in the periglacial areas, along the flat platforms, patterned ground and rocky outcrops slopes, which have more than 20% of their areas covered by vegetation (Table II). The waterlogged depressions, talus slope and paraglacial areas are moderately covered by vegetation (10 – 15%), and the marine terraces, and volcanic stacks are the lesser vegetated areas (< 10%) (Table II).

The moss carpet subformation is the most extensive vegetation class, covering 7% (11 ha) of the total area. In the northern sector of HP,

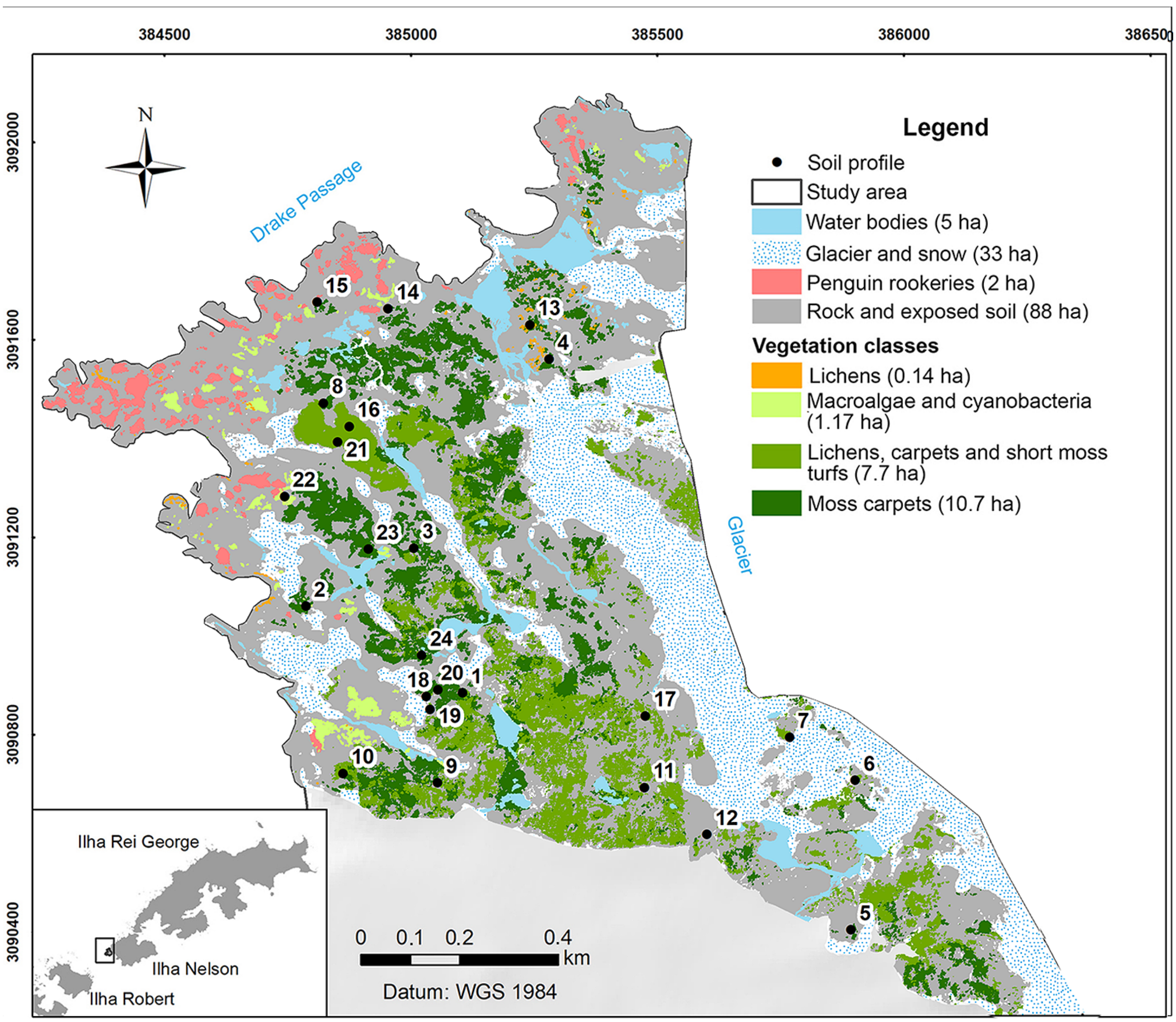

Figure 6. Vegetation class map of the northern sector of Harmony Point, Nelson Island, Maritime Antarctica.

this subformation forms extensive carpets of irregular to undulated surface and occurs in dry or humid and stable slopes (rocky outcrops slopes, Figure 7a) and in hydromorphic flat areas, where water accumulates (flat platforms, waterlogged depressions and marine terraces, Figure 7b, Table III), as also observed by Poelking et al. (2015). In the rocky outcrops, the *Sanionia uncinata* (Hedw.) Loeske, and *Sanionia georgicouncinata* (Müll. Hal.) Ochyra & Hedenäs predominates often intercalated with turfs of *Polytrichastrum alpinum* (Hedw.) G.L. Smith and *Polytrichum juniperinum* Hedw. In the waterlogged depressions predominates the *Sanionia* – *Warnstorfia* association and cyanobacteria often occurs. In marine terraces this subformation occur on more stable volcanic stacks, around channels, and lakes. Some lichens occur in more exposed areas, and musciculous and ornithocoprophilous lichens occur in areas with ornithogenic influence, where the ornithocoprophilous green algae *Prasiola crispa* (Lightfoot) Meneghini also occur.

The lichens, carpets, and short moss turf subformation represents 5% (7,72 ha) of the total area (Figure 6). This community corresponds to short, undulated or discrete moss turfs that predominates on protected and humid sites, such as rock crevices of the rocky outcrops and talus slope, and rocky, high, and flat terrains, like the flat platforms and paraglacial areas (Tables II and III). In the patterned ground areas (Figure 7c and 7d), the *Sanionia* – *Andreaea* association predominates, with *S. georgicouncinata* occurring in more humid areas than the *S. uncinata*. In the dryer areas of the borders of the patterned ground and top of rocky outcrops *Andreaea gainii* Cardot predominates, often along with musciculous lichens. In the rocky outcrops and talus slopes, the *Sanionia* – *Andreaea* occur associated with some *P. alpinum* and *Bryum archangelicum* Bruch & Schimp. turfs, and many fruticose lichens of the genus *Cladonia* and *Ochrolechia*, besides ornithocoprophilous lichens.

The lichens subformation predominates in the coastal areas and covers only 0.1% (0.14 ha) of the total area (Figure 6 and table II). This subformation corresponds mainly to crustose lichens, also occurring foliose and fruticose lichens and some moss species (Figure 7e). On the cliffs facing the sea (Figure 7f and table III), the halophilic lichen *Verrucaria* spp. predominates, due to its salt tolerance. It is also

Table II. **Percentage of area of the vegetation classes for each landform of the northern sector of Harmony Point.**

Landforms/Vegetation classes	Lichens	Lichens, carpets e moss turf	Moss carpets	Macroalgae and cyanobacteria	Total vegetation cover
	%				
Paraglacial areas	0	7.8	5.5	0	13.3
Waterlogged depressions	0	1.5	13.4	0.2	15.1
Talus slope	0.1	8.7	4.6	0.2	13.6
Rocky cliffs and volcanics stacks	0.5	0	1.2	0.5	2.2
Rock outcrops	0.2	6.7	18	1.8	26.7
Plataforms	0	9.7	15.5	2.2	27.4
Patterned groud	0	16.3	6.1	1.0	23.4
Marine terraces	0.3	0	8.1	1.5	9.9

found in the talus slope, waterlogged areas, and rocky outcrops of interior areas, evidencing the sea spray influence. The *Caloplaca – Rusavskia* (*Xanthoria*) association predominates in the coastal cliffs and volcanic stacks under guano influence and in the ornithogenic sites of the interior area. *P. crispa* also occur in ornithogenic areas, mainly in its lichenized form as *Mastodia tesselata* Hook. f. & Harv.

The macroalgae and cyanobacteria subformation represent less than 1% (approximately 1 ha) of the total area (Figure 6) and it predominates in the ornithogenic areas, such as rocky outcrops, convex slopes hill, patterned ground, and marine terraces (Tables II and III). The *P. crispa* (Figure 7g) predominates over areas of present penguin occupation, in the border of the rookeries where trampling is absent, and adjacent areas where the guano leachate reaches. *M. tesselata* is also found in these areas. The cyanobacteria *Nostoc* spp. (Figure 7h) and its lichenized form, *Leptogium puberulum* Hue, are found in saturated areas close to waterbodies.

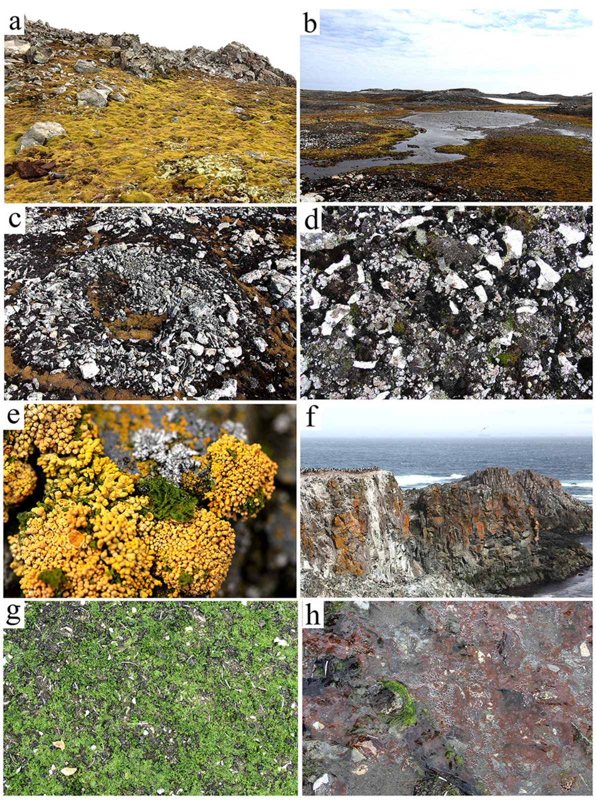

Figure 7. The vegetation classes of the northern sector of Harmony Point. a) Moss carpet on rock outcrop slopes; b) Moss carpet around waterlogged depressions; c) Lichens, carpets, and moss turfs on patterned ground; d) Community mainly composed of *A. gainii* associated with crustose and musciculous lichens, turfs of *P. alpinum* and *U. antarctica*; e) *C. regalis* (yellow) and macroalgae *P. crispa* (green); f) Association of *Caloplaca – Rusavskia* lichens on coastal rocky cliffs under the influence of Pygoscelis antarctica penguins. g) *P. crispa* in an area under ornithogenic influence of penguins; h) Cyanobacteria *Nostoc ssp*. in waterlogged depression.

Soil characterization

Applying the Kruskal-Wallis's test and the post-hoc Dunn's test (Table IV) for the physical attributes, we verify that only the difference in the gravel content was not statistically significant among the soil groups, and the differences in the coarse sand and silt contents were very significant ($p \leq 0.001$), indicating that the SRO and SMT groups were the most statistically different. In relation to the chemical attributes, the contents of K, Na, Ca^{2+}, Mg^{2+}, Fe, Cu, Mn, as well as CaO, Na_2O, P_2O_5, TiO_2, Fe_d, Al_d and Al_o were not significantly different among the soil groups. On the other hand, the water pH, pCEC, H+Al, TOC, TN, Al_2O_3, SiO_2 showed great statistical differences ($p \leq 0.001$) mainly among the SRO and SP groups.

PCA graphs were created indicating the most significant physical and chemical attributes of each soil group. The first two Principal Components (PC) presented eigenvalues above 1 and were selected for explaining the most part of the dataset variance. In relation to the physical attributes (Figure 8), PC1 explained 51.8% of the total dataset variance and is influenced by gravel, coarse sand, and silt. The PC2 explained 27.2% of the total dataset variance and is influenced by fine sand and clay. The

Table III. Representative species of the vegetation subformations of the northern sector of Harmony Point, Nelson Island, maritime Antarctica.

Subformation	Landforms and soil profiles	Species
Lichens	Vertical and horizontal faces of rocky cliffs and volcanic stacks; Debris on ornithogenic and/or hydromorphic soils of marine terraces and depressions (P4, P13, P14, P24); Rock outcrops and talus slope facing the coast (P8 and P16).	Crustose lichens: *Verrucaria sp., Acarospora macrocyclus* Vain. Foliose lichens: *Rusavskia elegans (L.) S.Y. Kondr. & Kärnefelt, Mastodia tesselata* Hook. f. & Harv.) Hook. f. & Harv. Fruticose lichens: *Caloplaca regalis (Vain.) Zahlbr, C. cinericola (Hue) Darb* and *Lecania brialmontii (vā). Zahlbr* and *Polycauliona candelaria (L.) Frödén, Arup, & Søchtin*.
Macroalgae and cyanobacteria	Macroalgae on the rock cliffs and rock outcrops under active ornithogenic influence (P1, P10, P14, P20, P22) and to a lesser extent in areas of inactive ornithogenic influence (P3, P5, P18, P23); Cyanobacteria in channels and waterlogged depressions.	Algae: *Prasiola crispa* (Lightfoot) Meneghini Cyanobacteria: *Nostoc* spp. Lichens: *M. tesselata* and *Leptogium puberulum* Hue
Lichens, carpets and moss turfs	Cryoturbated soils with dominance of patterned ground (P9, P10); Dry to slightly wet rocky outcrops (P1, P16, P19 and P21).	Mosses: *Sanionia uncinata* (Hedw.) Loeske, *S. georgicouncinata* J. Putzke & A. B. Pereira, *Andreaea gainii* Cardot, *A. depressinervis* Cardot, *Bryum archangelicum* Bruch & Schimp., *Polytrichastrum alpinum* (Hedw.) G.L. Sm., *Hennediella heimii* (Hedw.) R.H. Zander and *Ceratodon purpureus* Hedw. Brid; Lichens: *Cladonia borealis* S. Stenroos, *C. rangiferina* (L.) Weber ex F.H. Wigg., *C. metacoralifera* Asahina, *Ochrolechia frigida* (Sw.) Lynge, *Usnea antarctica* Du Rietz, *Buellia latemarginata* Darb. and *Cystocoleus niger Har.*
Moss carpets	Soils on stable rocky outcrops slopes and well-drained environments, dry to slightly moist, and carpets in waterlogged depressions (P2, P3, P5, P7, P8, P18, P23 and P24).	Mosses: *S. uncinata, S. georgicouncinata*, *P. alpinum*, *Polytrichastrum juniperinum* Hedw., *Warnstorfia fontinaliopsis* (Müll. Hal.) Ochyra, *W. sarmentosa* (Wahlenb.) Hedenäs, *B. archangelicum, Andreaea gainii* and *Hennediella heimii*; Lichens *C. borealis, C. rangiferina, C. metacorallifera, B. latemarginata*, *Verrucaria spp., Cystocoleus niger, A. macrocyclus*, *C. regalis, Rinodina petermannii* (Hue) Darb., *Psoroma hypnorum.*

SMT soils are mainly represented by gravel and coarse sand; the SP soils by clay, coarse sand, and gravel; and the SRO soils by fine sand and silt. The PC1 of the chemical attributes (Figure 9) explained 50.7% of the dataset variance and is influenced by H+Al, TOC, TN, and pCEC. The PC2 explained 27.7% of the total variance and is influenced by BS, PBS, and pH H_2O. The SRO group was more influenced by the H+Al, TOC, TN, pCEC and BS content. On the other hand, the SP and SMT were more explained by PBS and pH H_2O. The contribution of the available P was not significant for explaining the dataset variance between the soil groups once it presents high values for most of the samples.

Two main soil groups were possible to identify through the Spearman correlation matrix using the chemical variables (Figure 10). One group is related to the soils that presented a predominance of primary aluminosilicate and

Table IV. Kruskal-Wallis' and Dunn's tests of the physical and chemical attributes of the soils of rocky outcrops (SRO), soils of the platforms (SP) and soils of marine terraces (SMT) from the northern sector of Harmony Point.

Attributes		SRO	SP	SMT		Attributes		SRO	SP	SMT	
CF[1]	%				ns	Mn	mg kg^{-1}				ns
CS[1]	%	b	a	a	***	Fe	mg kg^{-1}				ns
FS[1]	%	b	a	a	**	Zn	mg kg^{-1}	b	a	ab	*
Silt	%	a	a	b	***	Al_2O_3	%	b	a	ab	***
Clay	%	a	a	b	**	CaO	%				ns
pH H_2O		b	a	b	***	K_2O	%	b	a	ab	**
P	mg kg^{-1}	ab	a	b	*	MgO	%	b	a	ab	**
K	mg kg^{-1}				ns	Na_2O	%				ns
Na	mg kg^{-1}				ns	SiO_2	%	b	a	ab	***
Ca^{2+}	$cmol_c\ kg^{-1}$				ns	TiO_2	%				ns
Mg^{2+}	$cmol_c\ kg^{-1}$				ns	P_2O_5	%				ns
Al^{3+}	$cmol_c\ kg^{-1}$	a	b	ab	*	SO_3	%	b	a	ab	**
H+Al	$cmol_c\ kg^{-1}$	b	a	a	***	Fe_d	%				ns
pCEC	$cmol_c\ kg^{-1}$	b	a	a	***	Al_d	%				ns
PBS	%	b	a	ab	**	Fe_o	%	b	a	ab	**
TOC	%	b	a	a	***	Al_o	%				ns
TN	%	b	a	a	***	Fe_p	%	b	a	ab	**
Cu	mg kg^{-1}				ns	Al_p	%	b	a	ab	*

[1] CF – coarse fraction; CS – coarse sand; and FS – fine sand.
*** p value <0.05; ** p value <0.01; *** p value <0.001; ns: p value > 0.05 (no significant).**

ferromagnesian minerals, as evidenced by the strong positive correlation (> 0.5) among pH H_2O, PBS, K_2O, SiO2, Al_2O_3, Fe_2O_3 and TiO_2. This group can be represented by the soils of the platforms (SP group). The second group is more related to soils that presented high organic matter content and ornithogenesis, as evidenced by strong positive correlations among TOC, TN, P_2O_5, SO_3, Al_d, and Fe_d. Strong negative correlations (< -0.5) between MgO, Fe_2O_3, SiO_2, Al_2O_3 and Al_d, Fe_d, P_2O_5, TN, TOC, and SO_3, highlight the relevance of the biological influence over these soils. This group corresponds to the soils of the rocky outcrops (SRO group) and the marine terrace (SMT group) due to the significant ornithogenic influence.

Soils of the rocky outcrops

This group represents the soils of the slopes of the rocky outcrops and encompasses the "Ornithogenic" Fibristels (1, 7, 8 and 18 soil profiles); the "Ornithogenic" Humigelepts (5, 6, 21 and 23 soil profiles), and the "Ornithogenic" Gelorthents (2, 3, 19, 20 and 22 soil profiles). The ornithogenic influence from present penguin rookeries were verified on profiles 2, 3 22 and 23 (Table I); and from abandoned penguin rookeries on profiles 8 and 21. Present petrel nest influence were found on profiles 1, 3, 5, 7, 18 and 20. Abandoned kelp gull nest were identified on profiles 6 and 19.

The mean soil depth was the highest among the other groups (Table V). The soil structure was mainly moderate medium granular. The main textural classes were sandy loam and sandy clay loam, due to the highest fine sand and silt contents, and second highest clay content. These soils presented a predominant dark brown color, the lowest mean pH values, and the highest mean Al^{3+}, H+Al, $Al_{sat,}$ TOC and TN contents compared with the other groups, which is mainly associated with a significant organic matter contribution and weathering of primary minerals. The SRO group also presented the highest mean BS content, such as Na, Ca^{2+} and Mg^{2+}, indicating nutrient accumulation by ornithogenic influence. However, the exchangeable P was the lowest among the groups, due to a weak to moderate ornithogenic influence mainly promoted by giant petrels. The PBS content was also the lowest, with soils predominantly dystrophic, which is explained by predominance of H+Al in the soil exchange complex.

The mineralogy of the coarse sand, fine sand and silt fractions were dominated by plagioclase, K-feldspar, and quartz. Apatite was also found in these fractions, which may exist with organic matter detritus, silicate minerals, and bone fragments (Tatur & Barczuk 1985, Almeida et al. 2021). The mineralogy of the clay fraction (Figure 11a) is mainly composed by phosphate minerals such as apatite, leucophosphite, struvite, minyulite and taranakite. These minerals indicate a highly phosphatized horizon, once their formation is related to precipitation of phosphate minerals from ornithogenic soil solutions that percolate through the soil (Almeida et al. 2021, Myrcha et al. 1985). Mica, plagioclase, K-feldspar and pyroxene were also identified in the clay fraction, due to cryoclastic process.

The strong correlation among Fe_d, Al_d, and P_2O_5 (Figure 10) corroborates with the existence of secondary Al and Fe phosphate minerals in the SRO. This group presented high contents of

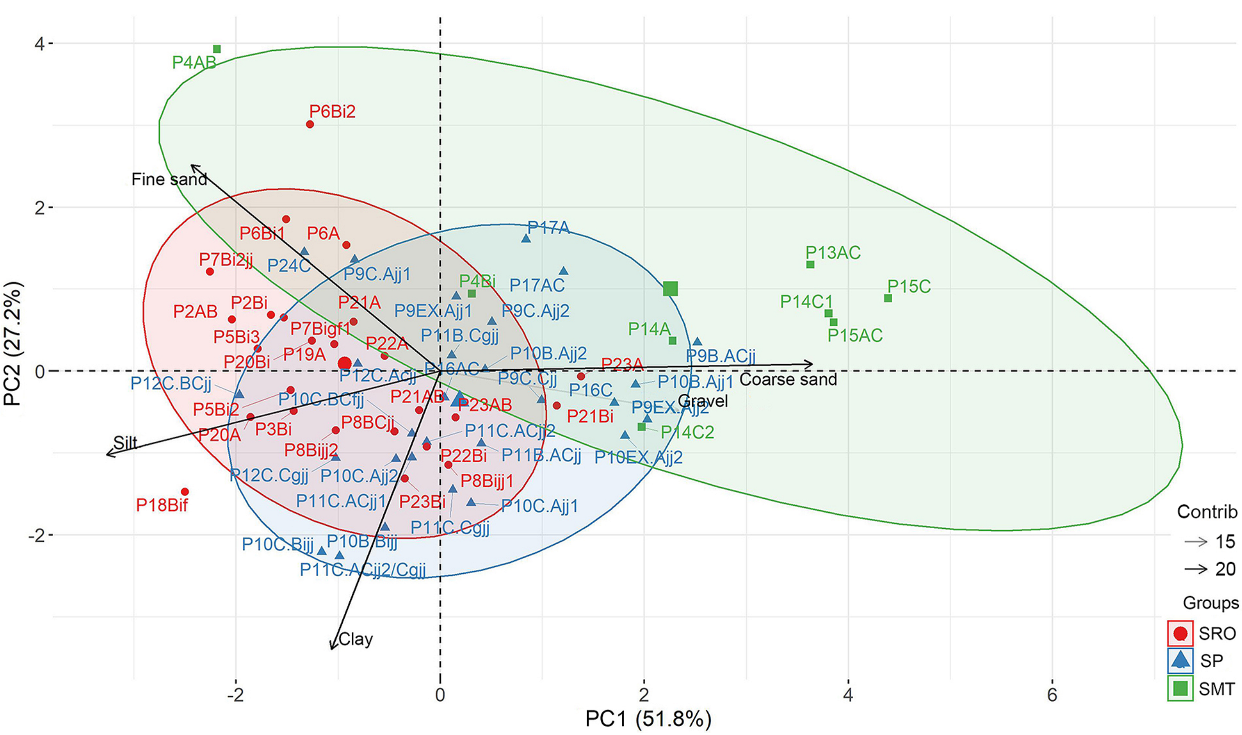

Figure 8. Principal component analysis of the physical soil attributes of the northern sector of Harmony Point.

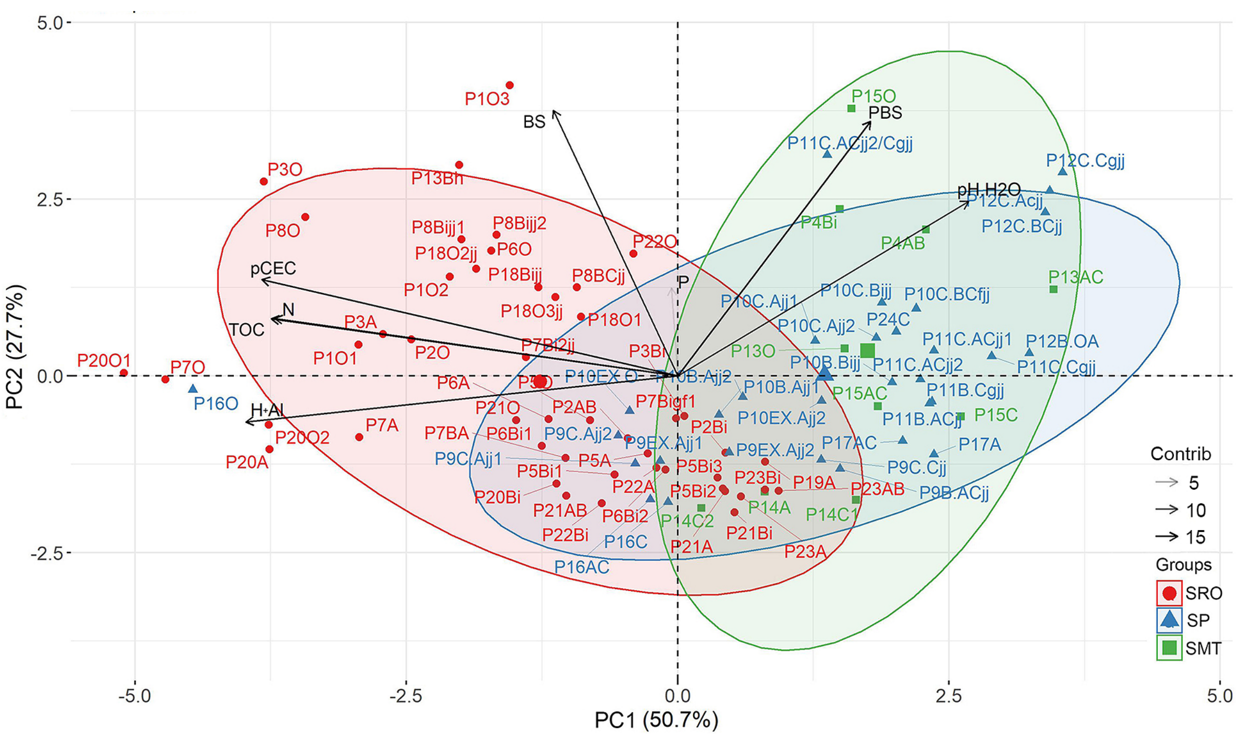

Figure 9. Principal component analysis of the chemical soil attributes of the northern sector of Harmony Point.

Fe and Al dithionite, oxalate, and pyrophosphate (Table VI), but the pyrophosphate values were higher than the oxalate, which indicates a predominance of organometallic compounds in the non-crystalline fraction of these soils, and, consequently, showing the important of the organic matter accumulation as a pedogenetic process. The P3 Bi horizon presented the highest content of Fe_d and K_2O (Table VII), high P_2O_5 and low Fe_o/Fe_d ratio, evidencing the presence of crystalline leucophosphite. The P8 Bi1 and Bi2 horizons presented high contents of CaO and P_2O_5, indicating the presence of apatite. High values of Al_2O_5, and P_2O_5 corroborates with the presence of taranakite in the P22 phosphatic vein.

Soils of the platforms

This group encompasses the soil profiles of the talus slope (P16 - Typic Gelorthent), located in the transition between the marine terraces and the platforms; of the patterned ground (P9 and P12 – Typic Haploturbel, P10 – “Ornithogenic” Umbriturbel, P11 Border – Aquic Haploturbel and P11 Center – Typic Aquiturbel), located in the periglacial areas; the waterlogged depression (P24 – Typic Gelaquents), in the upper platform; and paraglacial areas (P17 – Typic Haploturbel), close to the glacier. Only the P10 presented ornithogenic influence from an adjacent active penguin rookery.

The predominant soil structure is weak medium subangular blocky (Table V). Soil color is mostly brown (10YR 3/2), with some samples presenting greyish colors (hue 2,5Y), due to favorable hydromorphic conditions and the presence of phosphate minerals. The main soil texture classes were sandy loam and sandy clay loam. The soils presented the highest gravel (mean 57%) and clay content (mean 20%), which is mainly related to the accumulation of gravels in the borders of the patterned ground and of fine materials (silt and clay) in the center, due to the cryoturbation influence, which favors the

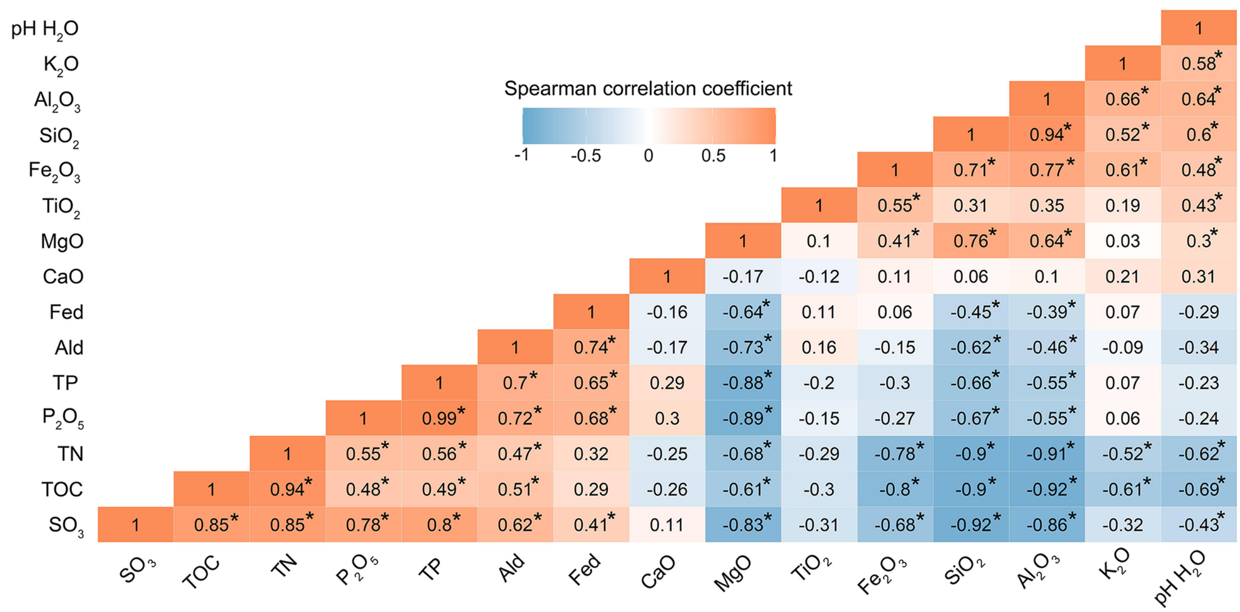

Figure 10. Spearmen correlation of the chemical soil attributes of the northern sector of Harmony Point. *p ≤ 0.05.

sorting and frost heave processes. The highest clay contents (approximately 31%) were found in the P10 BC and P11 AC/Cg horizons in the center of the patterned ground.

The SP presented the highest mean water pH content (Table V) among the groups and the highest value (6.79) among all soil samples at the surficial horizon of the P12 profile (Table VIII). This corroborates with the PBS content of that same horizon which reached the highest value (approximately 83%) among all soil samples. The available Fe mean values were the highest, which is related to a prevalent reducing condition, due to hydromorphism. The mean Cu content was the highest due to the ornithogenic influence on P10. Among the Turbel soils of the SP group, the P9 presented the highest values of TOC and TN (16 and 2.06 dag kg^{-1} respectively), due to the organic matter contribution by vegetation cover. The P10 presented the highest available P (10686.6 mg kg^{-1}), Cu (55.1 mg kg^{-1}), Mn (52.4 mg kg^{-1}), Zn (94.4 mg kg^{-1}) and S (73.8 mg kg^{-1}) contents due to an intense active ornithogenic influence (Table VIII). Added to that, the flat relief of the patterned ground area favor the accumulation of nutrients and water, enhancing the weathering processes of the parent material. The P11 and P12 presented only crustose lichens and very few mosses, once it is located in the transition from the paraglacial to periglacial environment and were characterized by higher water pH values and high clay content, due to the clayey and silty origin of glacial deposits. The P17, located in the paraglacial area, showed lower values (Table VIII) due to the absence of vegetation and ornithogenic influence, and the more recent exposition to non-glacial conditions.

Plagioclase, K-feldspars, pyroxene, and quartz were the main minerals found at the coarse sand, fine sand, and silt fractions of the ornithogenic soil of the patterned ground (P10). The clay fraction presented an assemblage of phosphatic minerals, such as leucophosphite, minyulite, taranakite and vivianite. Permanently wet and acidified conditions in subsurface, at the top of permafrost, favors the occurrence of vivianite (Myrcha et al. 1985). High contents of K_2O, Al_2O_3 and Fe_2O_3 (Table VII) indicate the presence of these minerals. Lower values of Fe_o and Al_o

Table V. Mean and standard deviation (SD) of the main morphological, physical, and chemical variables of the soils of rocky outcrops (SRO), soils of the platforms (SP) and soils of marine terraces (SMT) from the northern sector of Harmony Point.

Variables			SRO			SP			SMT	
	Unit	n*	Mean	SD	n*	Mean	SD	n*	Mean	SD
Color			10YR 3/3			10YR 3/2			5Y 4/1	
Texture			Sandy clay loam			Sandy loam			Sandy loam	
Structure			Moderate medium granular			Weak medium subangular blocky			Weak medium granular and single grains	
Depth	cm	29	52	19.34	30	46.2	15.54	10	44.1	15.38
CF*	%	29	40	29.84	30	57	23.84	10	48	30.64
CS*	%	29	29.17	9.62	30	39.27	10.42	10	59	28.44
FS*	%	29	23.8	8.09	30	17.6	8.26	10	15.5	18.7
Silt	%	29	27.65	7.1	30	22.97	6.53	10	12.5	10.35
Clay	%	29	19.62	4.98	30	20.5	5.42	10	12.9	4.95
pH H_2O		47	4.46	0.39	31	5.24	0.71	10	4.87	0.77
pH KCl		47	3.64	0.38	31	4.03	0.51	10	4.01	0.81
P	mg kg^{-1}	47	971.76	1163.55	31	1041.27	2087.87	10	1843.5	1854.27
K	mg kg^{-1}	47	177.57	79.31	31	164.19	89.76	10	143	40.6
Na	mg kg^{-1}	47	340.27	152.02	31	272.13	119.98	10	326.41	114.96
Ca^{2+}	cmolc kg^{-1}	47	6.64	5.59	31	4.74	5.14	10	5.98	5.3
Mg^{2+}	cmolc kg^{-1}	47	2.76	3.65	31	1.92	1.44	10	1.65	1.46
Al^{3+}	cmolc kg^{-1}	47	2.71	1.38	31	2.19	2.05	10	1.33	1.51
H+Al	cmolc kg^{-1}	47	32.04	10.78	31	15.78	9.79	10	11.05	7.3
BS	cmolc kg^{-1}	47	11.34	9.35	31	8.27	6.77	10	9.42	6.96
$_eCEC$	cmolc kg^{-1}	47	14.04	8.61	31	10.45	7.7	10	10.75	5.99
$_pCEC$	cmolc kg^{-1}	47	43.37	14.81	31	24.05	10.53	10	20.47	8.34
PBS	%	47	23.79	14.61	31	35.77	21.58	10	46.76	24.53
Al_{sat}	%	47	28.8	18.98	31	24.98	17.54	10	19.08	22.36
Na-SI	%	47	3.49	1.15	31	5.44	2.55	10	8.5	5.98
TOC	dag kg^{-1}	47	16.22	10.33	31	6.41	8.28	10	3.32	2.58
N	dag kg^{-1}	47	1.38	0.6	31	0.66	0.57	10	0.48	0.36
P-Rem	mg L^{-1}	47	16.64	13.75	31	17.19	11.21	10	31.96	11.97
Cu	mg kg^{-1}	47	11.7	11.08	31	13.73	14.52	10	12.84	6.59
Mn	mg kg^{-1}	47	9.04	11.73	31	15	15.33	10	22.47	25.82
Fe	mg kg^{-1}	47	368.55	190.73	31	400.21	190.3	10	321.06	143.42
Zn	mg kg^{-1}	47	11.38	18.02	31	13.53	27.04	10	19.70	24.76
S	mg kg^{-1}	35	34.51	32.66	30	13.7	18.90	11	81.94	122.80

*** CF – coarse fraction; CS – coarse sand; FS – fine sand; n – number of samples.**

were predominant, suggesting the presence of more crystalline phosphate minerals.

The non-ornithogenic soils of the patterned ground and the soil of the paraglacial area (P11, P12 and P17) presented the lowest contents of P_2O_5 and SO_3, and the highest contents of Al_2O_5, SiO_2, Fe_2O_5 and MgO (Table VII), indicating the predominance of silicate and ferromagnesian minerals. The mineralogy of these soils, originated from easily weatherable volcanic tuffs, presented chlorite, K-feldspar, plagioclase, pyroxene, amphibole, magnetite and quartz in the coarse sand, fine sand, and silt fractions. Treatments with Mg and K-saturation, glycerol solvation and heating of the clay samples confirmed the presence of chlorite, mica, hydroxy interlayered smectite and kaolinite (Figure 12).

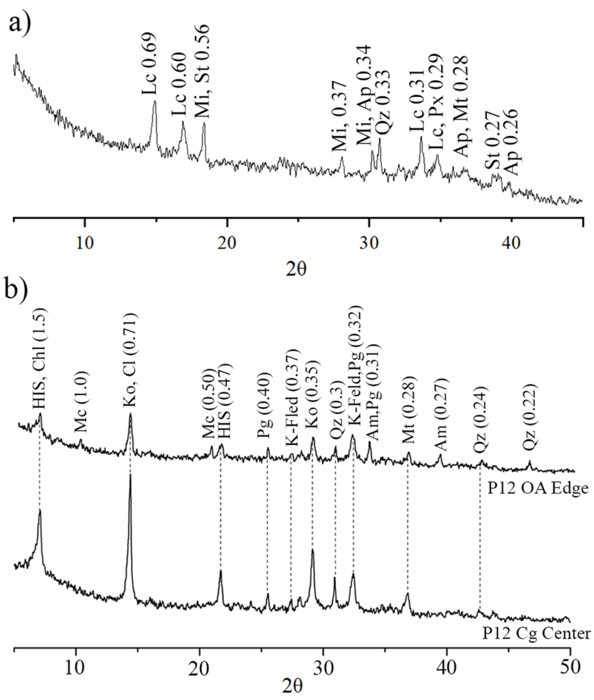

Figure 11. XRD pattern of clay fraction of a) an ornithogenic soil of a rocky outcrop (P3 Bi); and b) a non-ornithogenic soil of a patterned ground (P12 OA Edge and P12 Cg Center). Am – amphibole, Ap: apatite, Chl – chlorite; HIS – Hydroxy interlayered smectite, Ko – kaolinite, K-feld – K feldspar, Lc – Leucophosphite, Mc – Mica, Mt – magnetite, Pg – plagioclase, Px – pyroxene, Qz – quartz; and St – Struvite; d in nm.

These minerals have already been reported at MA soils (Simas et al. 2006, Jeong & Yoon 2001). Kaolinite was confirmed with the disappearing of the 1.02 nm peak at 550 ºC, as Simas et al. (2006) has also found in sulfate soils of MA. High contents of SiO_2 and Al_2O_3 (Table VII) corroborate the presence of kaolinite. K-feldspar, plagioclase, amphibole, and quartz were also found in the clay fraction (Figure 11b). Weatherable primary minerals in clay fraction are common in soils of Antarctica due to the dominance of physical weathering, related to cryogenic processes (Mendonça et al. 2013, Navas et al. 2008).

Soils of the marine terraces

This group encompasses the soils of the marine terraces, located in the first level (P15 – "Ornithogenic" Gelaquent); the second level (P4 – "Ornithogenic" Gelorthent and P14 – "Ornithogenic" Gelaquent, respectively); and the third level (P13 – Typic Cryopsamment). The penguin rookeries predominate in the marine terraces, where we found present (P14 and P15) and past (P4) penguin influence.

The soils are shallow, presenting an average depth of 44 cm (Table V). The predominant color is dark grey (5Y 4/1), indicating hydromorphic conditions and organic matter influence. The soil structure varies between weak medium granular and single grains. The coarse sand content presents the highest values (mean 59%) and a high content of gravels and pebbles are found in the lowest levels (P14 and P15) marine terraces. Sand, pebbles, and gravels are characteristic of this environment, due to fluvioglacial deposition, marine action, and physical weathering of the volcanic stacks.

The SMT group presented intermediate acidity, with pH in water values ranging from 3.9 to 5.8. The PBS mean value was the highest (46.76%) and most soil profiles (P4, P13 and P15) were eutrophic, with PBS value reaching

Table VI. **Fe and Al contents extracted by DCB, amonium oxalate and sodium pirofosfate methods of selected soil samples and mean and standard deviation (SD) for each soil group (soil of the rocky outcrops – SRO, soils of the platforms – SP, and soils of marine terraces – SMT).**

Sample		Fe_d	Fe_o	Fe_p	Al_d	Al_o	Al_p	Fe_o/Fe_d	Al_o/Al_d
		dag kg^{-1}							
P3A		1.2	0.9	1.4	0.6	0.5	1.1	0.8	0.7
P3Bi		2.7	1.3	1.7	1.6	1.4	1.8	0.5	0.9
P6A		1.8	1.4	2.5	1.4	1.2	2.5	0.8	0.9
P6Bi1		2.4	2.1	3.5	1.7	1.4	3.2	0.9	0.8
P6Bi2		2.3	2.0	3.5	1.5	1.3	2.7	0.9	0.9
P8Bijj1		1.7	1.0	0.9	0.8	0.4	0.9	0.6	0.5
P8Bijj2		1.8	1.2	1.0	1.0	0.8	0.9	0.7	0.8
P8BCjj		2.5	1.9	1.2	1.2	0.8	1.0	0.8	0.7
P10Ajj2-O*		1.8	1.0	1.0	1.0	0.7	1.0	0.5	0.7
P10Ajj1-E*		1.3	0.9	0.9	0.8	0.7	1.0	0.7	1.0
P10Bifjj-E*		2.2	1.0	1.0	1.6	1.2	1.0	0.4	0.8
P10Ajj1-C*		1.8	1.2	0.8	1.5	1.7	1.1	0.6	1.1
P10Bijj-C*		2.2	1.1	0.8	1.9	2.1	1.2	0.5	1.1
P10BCfjj-C*		2.1	1.1	0.9	1.8	1.5	1.2	0.5	0.8
P11ACjj2/Cgjj-C*		1.4	0.9	0.6	0.2	0.5	0.8	0.6	2.2
P11Cgjj-C*		0.6	0.5	0.4	0.2	0.3	0.7	0.8	1.3
P12OAjj-B*		0.6	0.6	0.4	0.3	0.4	0.3	1.0	1.3
P12Cgjj-C*		0.8	0.7	0.5	0.4	0.5	0.3	0.9	1.2
P12BCjj-C*		1.3	1.0	0.7	0.5	0.7	0.4	0.8	1.3
P14A		1.2	1.0	1.6	0.3	0.4	0.8	0.9	1.4
P14C2		2.5	2.6	3.3	1.6	1.6	2.7	1.1	1.0
P17A		0.9	0.9	1.0	0.4	0.5	0.9	0.9	1.0
P17AC		2.4	2.3	2.6	0.8	0.7	1.2	1.0	0.9
P19A		1.8	1.3	1.4	1.2	1.0	1.6	0.7	0.8
P20A		1.8	1.1	2.1	1.9	1.5	3.1	0.6	0.8
P20Bi		2.2	1.2	1.5	2.3	1.8	2.7	0.6	0.8
P22A		2.2	1.3	1.8	1.2	0.8	1.0	0.6	0.6
SRO	n*	12	12	12	12	12	12	12	12
	Mean	2.0	1.4	1.9	1.4	1.1	1.9	0.7	0.8
	SD	0.4	0.4	0.9	0.5	0.4	0.9	0.1	0.1
SP	n*	13	13	13	13	13	13	13	13
	Mean	1.5	1.0	0.9	0.9	0.9	0.9	0.7	1.1
	SD	0.6	0.4	0.6	0.6	0.6	0.3	0.2	0.4
SMT	n*	2	2	2	2	2	2	2	2
	Mean	1.8	1.8	2.5	1.0	1.0	1.7	1.0	1.2
	SD	0.9	1.1	1.2	0.9	0.8	1.3	0.1	0.2

***Parts of the patterned ground: O – Outer; B – border; C – center; n – number of samples.**

81% at the P13 AC horizon. Na-SI and available S presented the highest mean values (8.5% and 91.94 mg kg^{-1} respectively), due to saline spray and eolian deposition and/or inundation by seawater (Prietzel et al. 2019). Available P, P-Rem, and Zn presented the highest mean contents (1843.5 mg kg^{-1}, 31.96 mg L^{-1} and 19.7 mg kg^{-1} respectively) among the groups mainly at the surface of most soil profiles, due to the current ornithogenic input (Rodrigues et al. 2021b). Besides the dense vegetation cover, the TOC values were the lowest (3.32 dag kg^{-1}), due to lower clay contents. P14 presented high Fe_o/Fe_d, Fe_p and Al_p, indicating the presence of amorphous minerals and organometallic complexes of Fe and Al (Table VI).

Table VII. Mean and standard deviation (SD) results of the FRX analysis for selected soil samples.

Sample		P_2O_5	CaO	MgO	K_2O	SiO_2	Al_2O_3	Fe_2O_3	TiO_2	SO_3
		%								
P3A		1.28	2.75	0.63	0.22	17.45	3.97	4.18	0.83	0.56
P3Bi		6.58	2.68	0.15	1.25	21.11	7.44	5.81	0.89	0.47
P6A		2.39	2.42	0.58	0.21	18.14	6.07	4.46	0.85	0.42
P6Bi1		3.53	2.31	0.56	0.24	19.65	6.85	5.18	0.96	0.37
P6Bi2		3.34	3.1	0.52	0.29	25.16	7.79	5.97	1.1	0.28
P8Bijj1		9	10.75	0.17	0.43	13.7	3.29	3.37	0.35	1.17
P8Bijj2		10.09	12.16	0.2	0.45	12.34	3.44	3.2	0.37	1.15
P8BCjj		10.71	11.94	0.06	0.61	17.42	4.79	5.05	0.54	0.8
P10Ajj2-O*		3.33	2.52	0.61	0.86	30.96	8.54	5.14	0.72	0.36
P10Ajj1-E*		2.03	2.41	0.64	0.91	29.17	9.93	5.31	0.66	0.32
P10Bifjj-E*		8.27	3.01	0.45	1.39	29.76	10.96	7	1.04	0.35
P10Ajj1-C*		7.89	5.32	0.42	1.17	29.06	9.94	5.82	0.87	0.42
P10Bijj-C*		9.2	5.02	0.21	1.44	24.38	9.75	5.74	0.96	0.46
P10BCfjj-C*		6.84	3.75	0.33	1.05	27.79	9.87	6.27	1.07	0.36
P11ACjj2/Cgjj-C*		0.32	3.54	1.99	1.8	39.27	15.61	6.28	0.7	0.01
P11Cgjj-C*		0.37	3.59	2.13	0.97	47.72	14.14	6.01	0.67	0.03
P12OAjj-E*		0.44	3.78	1.48	0.64	43.98	11.12	5.66	0.93	0.03
P12Cgjj		0.47	3.4	1.36	0.67	42.35	12.22	5.63	0.76	0.03
P12BCjj		0.68	3.63	1.24	0.5	36.12	10.65	5.87	0.93	0.05
P14A		1.46	3.46	1.49	0.41	35.04	9.4	5.67	0.72	0.25
P14C2		5.23	3.09	0.75	0.5	27.3	9.16	6.15	0.55	0.34
P17A		1.29	4.35	0.88	0.72	39.59	10.82	6.68	1.24	0.11
P17AC		2.59	3.08	0.75	0.72	35.29	9.79	6.12	0.83	0.11
P19A		1.47	2.9	0.52	0.36	22.31	7.84	5.53	0.95	0.36
P20A		3.49	1.88	0.44	0.18	9.72	4.53	3.35	0.53	0.63
P20Bi		8.92	6.93	0.11	0.45	19.31	7.2	4.86	0.64	0.63
P22A		5.38	2.53	0.11	0.85	26.47	8.3	5.37	0.8	0.35
SRO	n*	12	12	12	12	12	12	12	12	12
	Mean	5.34	5.01	0.32	0.46	18.79	6.00	4.82	0.76	0.60
	SD	3.35	3.97	0.22	0.30	4.82	1.78	1.04	0.25	0.29
SP	n*	13	13	13	13	13	13	13	13	13
	Mean	3.36	3.65	0.96	0.99	35.03	11.03	5.96	0.88	0.20
	SD	3.41	0.86	0.63	0.38	7.16	1.94	0.52	0.18	0.17
SMT	n*	2	2	2	2	2	2	2	2	2
	Mean	3.35	3.28	1.12	0.46	31.17	9.28	5.91	0.64	0.30
	SD	2.67	0.26	0.52	0.06	5.47	0.17	0.34	0.12	0.06

***Parts of the patterned ground: O – Outer; E – edge; C – center; n – number of samples**

Table VIII. Selected physical and chemical attributes of the soils of the patterned ground area, northern sector of Harmony Point, Nelson Island.

Sample	Depth	CS	FS	Silt	Clay	pH H_2O	P	Al^{3+}	SB	pCEC	V	TOC	NT	Cu	Mn	Fe	Zn	S
	cm	dag kg^{-1}					mg kg^{-1}	kg^{-1}			%	dag kg^{-1}		mg kg^{-1}				
P9A1-O*	0-18	34	29.6	20.8	15.6	4.44	100.9	3.15	4.38	26.98	16.2	15.97	1.00	2.92	2.6	443.2	1.18	41.1
P9A2-O*	18-40	53.9	12.2	12.3	21.6	5.05	222	2.86	3.44	26.04	13.2	11.30	0.79	5.19	2.1	574.5	0.85	2.1
P9AC-E*	0-40	60	13.8	10.9	15.3	4.75	178.4	2.66	3.38	17.68	19.1	4.09	0.38	2.12	2.1	487.5	0.8	2.1
P9A1-C*	0-10	21.6	40.5	21.4	16.5	4.44	104.7	3.05	3.97	27.67	14.3	15.59	1.26	3.74	1.9	529.4	1.19	56.2
P9A2-C*	10-35	37.7	25.3	20.9	16.1	5.02	120.8	2.56	3.61	28.11	12.8	12.47	2.06	4.37	1.7	627.6	0.77	6.9
P9Cjj-C*	35-45	47.1	12.8	21.3	18.8	5.1	490.9	2.76	3.08	21.58	14.3	4.91	0.39	7.98	3.5	880.5	0.43	0.8
P10O-O*	0-6	40.4	20.3	15.4	23.8	4.4	510.1	2.86	8.26	31.96	25.8	11.69	1.46	5.98	5.1	261.4	5.03	30.5
P10A2-O*	23-41	49.5	13.7	17.5	19.2	4.87	10686.6	0.39	21.67	38.07	56.9	6.62	1.33	11.94	34.4	26.6	58	73.8
P10A1-E*	6-23	54.7	12.8	14	18.5	4.48	442.2	2.46	8.08	27.88	29	7.79	0.96	8.92	9.8	312.5	6.03	7.4
P10A2-E*	23-41	42.1	18.3	21	18.6	5.1	561.4	1.67	7.11	27.11	26.2	9.55	0.97	18.94	34.8	336.6	13.37	3.7
P10Bi-E*	52+	30.2	10.4	31.6	27.7	5.65	796.8	1.28	5.44	17.14	31.7	2.65	0.73	17.41	22.7	358.7	12.92	0.8
P10A1-C*	0-6	39.3	8.7	26.2	25.8	5	4301.8	1.08	8.68	24.48	35.5	4.21	0.64	53.7	37.3	237.8	94.4	15.5
P10AB-C*	6-21	35.6	14.5	24.5	25.4	5.58	3394	1.28	7.31	20.81	35.1	3.66	0.57	55.1	48.3	279.3	76.9	3.6
P10Bi-C*	21-53	30	9.7	28.3	31.9	5.66	3495.3	0.69	9.21	21.11	43.6	3.43	0.72	51.2	52.4	183	83.4	0.8
P10BCjj-C*	53-77	36.5	12.6	30.4	20.5	5.82	1900.5	0.69	9.74	20.94	46.5	2.34	0.53	30.71	26.1	276.2	45.1	6.4
P11AC-E*	0-20	38.7	12.9	27.1	21.3	5.38	217.4	2.17	5.19	15.09	34.4	2.73	0.24	9.78	4.9	516.2	0.88	0.8
P11Cg-E*	20-40	41.3	19	21.9	17.9	5.37	148.2	1.48	5.18	14.48	35.8	2.73	0.28	7.49	6.9	516.8	0.83	3.1
P11AC1-C*	0-10	37	12	27.7	23.3	5.62	189.7	3.05	8.79	19.69	44.6	1.95	0.23	13.75	8.2	421.1	1.34	2
P11AC2-C*	10-20	38.2	14.1	24.2	23.5	5.6	188.8	1.58	6.61	18.01	36.7	3.11	0.30	15.02	9	668	0.71	2.5
P11AC/Cg-C*	10-40	29.5	9.7	29.2	31.6	5.18	41.6	10.64	34.85	47.65	73.1	0.23	0.02	2.33	10	100.7	1.85	19.3
P11Cg-C*	20-40	36.1	11.5	27.1	25.3	5.37	162.3	3.35	7.35	13.55	54.2	0.39	0.04	8.29	2	177.9	0.91	15.4
P12OA-E*	0-30	55.9	15.4	12.5	16.2	5.8	155.6	0.3	5.05	9.45	53.4	1.17	0.10	4.03	15	281.6	0.97	8.9
P12Cg-C*	0-25	29.7	16.6	28.2	25.5	6.79	258.9	0	17.47	21.07	82.9	0.93	0.09	6.21	22	351.8	0.98	0.8
P12AC-C*	0-25	30.8	22.2	28.5	18.5	6.7	195.9	0	16.14	20.34	79.4	1.48	0.15	11.42	28.9	446.6	1.18	1.2
P12BC-C*	0-25	24	20.2	35.6	20.2	6.64	187.1	0	14.37	19.07	75.4	1.72	0.16	7.87	33.7	426.8	1.24	0.8
P17A	0-42	41.6	31.5	14.5	12.4	5.35	355.2	1.18	2.06	10.66	19.3	2.34	0.27	4.69	2.8	388.7	0.71	9.5
P17AC	42-60	50.9	17.6	23.2	8.3	5.44	388.2	1.38	3.23	16.53	19.6	2.02	0.26	7.17	2.9	637.3	0.57	5.4

***Parts of the patterned ground: O – Outer; E – edge; C – center of the pattern.**

DISCUSSION

Pedogeoenvironmental relationships

Due to the proximity to the ocean, penguins and other marine animals use the coastal environment for reproduction. Radiocarbon dating of the marine terraces of different parts of the SSI (Barsch & Mäusbacher 1986, Del Valle et al. 2002, Hall 2010, Hallet 2013, John & Sugden 1971, Simms et al. 2011, Tatur et al. 1997), showed that the marine terraces lower than 6 m of altitude are no older than 802 years BP and the marine terraces of 8-12 m of altitude have, approximately, 1100 to 2050 years BP. This indicates a recent occupation of these environments by the fauna, especially the penguins. In the northern sector of HP, penguin rookeries predominate in the volcanic stacks on marine terraces and close to the coastal cliffs. The soils of the marine terraces (SMT group) showed clear signs of the influence of penguin

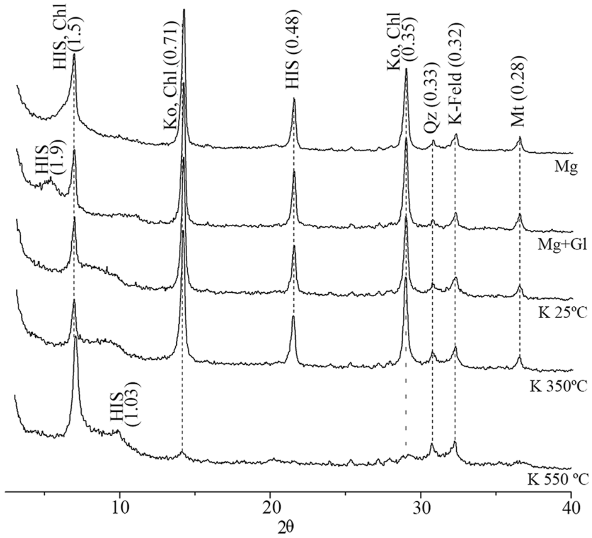

Figure 12. XRD patterns from the P12 Cg horizon of the center of the patterned ground. Chl – chlorite; HIS – hidroxy interlayered smectite; Ko – kaolinite; K-feld – K feldspar; Qz – quartz; and Sm – smectite; d in nm.

guano, which is rich in P and bases (K, Ca^{2+} and Mg^{2+}). The high Na-SI content of these soils are explained by the saline spray, which contribute to the soil eutrophication as also identified in other marine terraces areas in the SSI (González-Guzmán et al. 2017). The mineralogy of P14 corroborates with the recent ornithogenic influence, with a dominance of poorly crystalline phosphate minerals. Despite the abundant vegetation cover, with the predominance of moss carpets, the average TOC content of these soils was the lowest, due to the high sand content. The high contents of gravel and coarse sand in these soils indicate deposition by fluvial processes and influence of the parent material on pedogenesis, since andesitic basalt is more resistant to physical weathering than the volcanic tuffs, for example, also found in the area (Rodrigues et al. 2019). The repeated presence of rolled pebbles along the profile indicates past marine influence caused by the abrasive action of waves.

The influence of winds in coastal and transitional environments is evidenced by ventifacts on rocks and the prevalence of crustose lichens found in drier environments. The stability evidenced in lee-facing rocky outcrops in these environments favored vegetation and soil development. P8, located on a rocky outcrop talus in the transition zone, corresponded to the Fibristel soil class and had a dense vegetation cover (moss carpet subformation), with finds of former penguin rookeries (pebbles and feathers). The pedogenetic development of this soil was evidenced by high clay content, low pH, and contents of available and total P increasing at depth, as well as Fe_d, which indicates the presence of very crystalline Fe-phosphate minerals. TOC content at the surface is high and increases in the horizons above the permafrost due to cryoturbation.

The presence of biological activity is an important factor that contributes to the establishment of the periglacial environment, once it promotes stability and chemical transformations to the unconsolidated material, and, consequently, favors the development of pedogenetic processes (Abakumov 2018, Machado et al. 2019). The cryoplanation platforms of the northern portion of HP had a large area of patterned ground. Patterned ground is the main evidence of cryoturbation in Antarctic soils (Balks et al. 2013, Simas et al. 2015) and have already been extensively mapped in the SSI (Francelino et al. 2011, López-Martínez et al. 2012, Michel et al. 2014, Rodrigues et al. 2019). In patterned ground area more distant from the glacier, located in the periglacial environment, the importance of the biological factor on soil development and landscape stabilization is clear. In this area, the patterned ground showed well-defined circles, due to the flat relief, and availability of water and fine material; and a well-established vegetation, which indicates a longer exposure time to periglacial processes and biological influence. In the transition to the paraglacial environment, the shapes of the patterns were not well defined, and the vegetation cover was minimal, becoming absent closer to the glacier. In these areas, the steepest slope favored the occurrence of striated pavements, due to solifluction and frost creep processes, and less differentiation of the soil fraction in the formation of the pattern, indicating incipient sorting process.

The soils of rocky outcrops (SRO soil group) of the periglacial areas showed the highest degree of pedogenetic development. Most of these rocky outcrops showed, both past and present, ornithogenic influence from penguins, giant petrels, and kelp gulls, which favored soil development. These sites are considered hotspots of nutrient and vegetation micro-oasis in Antarctica ecosystems (Lopes et al. 2022). The chemical and mineralogical transformations in soil promoted by guano decomposition are responsible to accelerate chemical weathering of the rock material, increasing the concentration of P, Ca, K, and organic matter in soil, which favors the vegetation colonization (Schmitz et al. 2020a, b, 2022). Most of the ornithogenic rocky outcrops presented a dense vegetation cover, predominated by mosses. The vegetation cover promotes more stability to the outcrop slope, preventing erosion and gravitational process, which favor pedogenesis and determine soil attributes and functioning (Durán et al. 2021). In the rocky outcrops, weathering occurs in the rock crevices, where water and guano accumulates and where there is the existence of a pre-weathered saprolite. The water available by the active layer dynamic in the rocky outcrop Gelisols favors fungal diversity and distribution (Da Silva et al. 2020), which helps enhance weathering and, consequently, pedogenesis in the rock crevices. As a result, the rocky outcrops soils were more acidic, dystrophic, and presented crystalline secondary phosphate minerals, which indicate a long period of pedogenesis.

The rocky outcrops are very important for bird colonization in Antarctic coastal areas (Lopes et al. 2022). Currently, in the coastal areas of HP, the rocky outcrops, also called volcanic stacks, are occupied by penguins' colonies, and in the interior by flying birds, especially giant petrels. The abandoned penguin rookeries of the interior and transition area of the platforms are mainly explained by the glacio-isostatic uplift of the SSI. The penguins abandoned these sites when rocky outcrops became inaccessible (too steep) after glacio-isostatic raising (Tatur et al. 1997). So, it is possible that many rocky outcrops of the high platforms may also have been occupied by penguins when these areas were closer to the coast. In recent decades, the growing glacial retreat, linked to climate change, has exposed new areas, which impacts local ecosystems, and makes these locations available for penguin occupation (Pudełko et al. 2018). The Humigelepts (P5, P6, P21 and P23) were considered the most developed soils of the northern sector of HP and all of them presented past and/or present ornithogenic influence. The P21 and P23 are in an area of hills, considered as more developed rocky outcrops, in the high platform close to the transition talus slope. These soils presented past and present ornithogenic influence of penguins, respectively. The P5 and P6 are influenced, respectively, by present petrel and abandoned gull nests. Despite being closer to the glacier, these areas corresponded to high rocky outcrops, which are much used for flying birds for nesting and protection. In this regard, there is a close relation among landforms, time and ornithogenic activity, which directly influence the soil development.

Main soil forming processes

The major pedogenetic processes identified in the soils of the northern sector of HP were phosphatization, organic matter accumulation, and cryoturbation. Phosphatization is a pedogenetic process that has been widely described in the Maritime Antarctic (Abakumov et al. 2021b, Michel et al. 2006, Rodrigues et al. 2021b, Schaefer et al. 2008, Simas et al. 2007, Tatur & Myrcha 1984). The large availability of water on the islands in this region is an important factor in this process, favoring reactions between the N- and P-rich penguin guano and the rocky substrate. According to Schaefer et al. (2008), phosphatization in the fractures and cleavages of the large rocks occurs through the reaction between the soil solution (rich in guano leachates) and the rock. This removes Si from the structure of the rock minerals and causes P to react with Al and Fe, producing various forms of amorphous and crystalline phosphate minerals.

At the northern portion of HP, it was observed that in areas of current guano deposition, the soil surface layers presented higher values of pH, PBS, and available P due to direct nutrient input. As guano decomposes, its products are leached laterally and vertically along the soil profile. Soils of guano leachates influence had considerable PBS contents, higher available P content at depth, and high acidity, resulting in the formation of amorphous and/or crystalline phosphate minerals. Lopes et al. (2021) also identified the importance of seabirds activity in promoting sea-land bio-transfer of nutrients, which favors soil fertilization and water ornitheutrophication. During mineralization of guano, the ammonium (NH^{4+}) present in guano, can be converted to nitrate through the nitrification process which strongly contributes to soil acidification (Myrcha et al. 1985, Otero et al. 2018).

Vegetation was abundant in the north of HP and is the primary source of organic carbon uptake into the soils. Organic matter accumulation is also an important process of soil formation in the maritime Antarctic (Bockheim 2015). Organic matter accumulation is favored by low temperatures, which retard the decomposition rate of organic matter by saprophytic microorganisms and favor melanization, that corresponds to the darkening of soil horizons due to organic matter accumulation (Bockheim & Ugolini 1990). As highlighted by Garrido-Benavent et al. (2020), the development of soil and the colonization of cryptogamic organisms in polar regions are facilitated by bacterial, fungal, and algal communities, which act as pioneers in the primary succession process. In general, the surface horizons identified at HP were thick and the colors ranged from dark brown to black, exhibiting accumulation of organic matter in a varied degree of decomposition. The profiles with organic horizons corresponded to folic or folistic horizons (according to WRB/FAO and Soil Taxonomy, respectively) and were classified as Fibristels, due to the domain of fibric organic material, little humified. The mineral horizons that presented a supply of organic matter, corresponded to umbric horizons, since the drainage restriction for these horizons occurs seasonally and has short duration. The soil profiles with umbric horizons were classified as Umbriturbels. Most of the soil profiles obtained a humic qualifier, according to the WRB/FAO, due to the considerable TOC content.

Organic matter was fundamental in promoting the soil development in the northern sector of HP. Such development was observed through the formation of blocks and granules structures, promoted by the aggregation provided by the organic matter; the greater active, exchangeable and, mainly, potential acidity, indicating a greater buffering capacity of the soils; and higher levels of micronutrients. Organic matter also contributed to the formation of Fe and Al organometallic complexes, as pointed out by the pyrophosphate results for the rocky outcrops ornithogenic soils. This means that most of the non-crystalline mineral fraction of ornithogenic soils corresponds to organometallic complexes, as also pointed out by Simas et al. (2007) and Rodrigues et al. (2019). Besides that, vegetation also influences the thermal regime of the soils. Vegetation cover has a greater thermal insulating capacity, attributed to a longer duration of the snowpack, preventing temperatures change near the soil for long periods, which influence the thaw and freezing cycles of the active layer and, consequently, in the cryoturbation process (Schaefer et al. 2017). In areas with sparse vegetation cover, such as the James Ross Island, the heat transport between air and ground is fast, favoring the cooling of the ground (Ambrožová et al. 2020). Andrade et al. (2018) identified a relation between solar radiation and vegetation distribution at the Fildes Peninsula and Ardley Island, and suggested that mosses demand more solar radiation than lichens.

Cryoturbation is a pedogenetic process widely found in Antarctic soils affected by permafrost (Bockheim & Tarnocai 1998). At the northern portion of HP, nine of the 24 profiles collected showed permafrost, at an average depth of 36 cm, as also identified by Rodrigues et al. (2019). Organic soils affected by permafrost were classified as Fibristels and patterned ground soils were classified as Umbriturbels, Haploturbels and Aquiturbels. Among the evidences of cryoturbation, we found accumulation of organic matter in permafrost, oriented stones, irregular horizons and migration of thinner material in depth. This last evidence corresponds to the process called pervection, which is associated with sorting, resulting in the accumulation of fine material (silt and clay) at depth and segregation of coarse material (coarse fraction, sand) at surface.

Fibristels showed less evidence of cryoturbation, which is related to the accumulation of organic matter in the surface layers, promoting damping of movements caused by cryoturbation. In contrast, the patterned ground soils showed clear evidence of this process since they are typical features of cryoturbation. We observed that the location of the patterned ground soils at flat areas favors the accumulation of water and, consequently, increases the cryoturbation process. Likewise, the higher content of fine material contributed to the formation of the patterns. The presence of primary minerals in the clay fraction in the maritime Antarctic soil are commonly explained by cryoclasty, due to daily freeze-and-thaw cycles (Balks et al. 2013). P9 stoods out for the greater contribution of organic matter instead of clay to the formation of the pattern, and P10 presented a strong ornithogenic influence, whose secondary phosphate minerals were the main contributors to the high clay content of the soil. P11 and P12 presented higher clay content, which were composed by ferromagnesian minerals and phyllosilicates, such as chlorite, smectite, hidroxy-interlayered smectite, and kaolinite. P17 was the only soil with a striated pattern, resulting from the solifluction process.

The occurrence of chlorite, smectite, and kaolinite was noted elsewhere in MA. Some studies (Jeong & Yoon 2001, Lee et al. 2004) associate the origin of chlorite with rocks that have undergone weak metamorphism and the origin of smectite and kaolinite with paleohydrothermalism associated with magmatic intrusions and subsequent volcanism. Blume et al. (2002) noted corroded surfaces of pyroxenes, mica, and feldspars, and the presence of illite and smectite in the clay fraction in several soils on King George Island, which they linked to the occurrence of chemical weathering promoted by water availability during hot summer and acidification promoted by organic matter and guano mineralization. Other authors (Lopes et al. 2019, Simas et al. 2006, Siqueira et al. 2022) linked the greater chemical weathering in MA to the sulfurization process that occurs in sulphate acidic soils where kaolinite also occurs. It is possible that the origin of chlorite and kaolinite in the northern sector of HP is related to paleohydrothermalism of volcanoclastic rocks, and the origin of smectite with hydroxy interlayers is related to chemical weathering of smectites from pre-weathered saprolite caused by polymerization of Al^{3+} forms in soil from aluminosilicates such as plagioclase (Simas et al. 2006).

The saprolite observed in rock crevices of the rocky outcrops was formed during a warmer and wetter past climate, which persisted until the Paleogene period (Le Roux 2012). The transition of Antarctica continent to a polar condition occurred in the Miocene epoch (Armienti & Baroni 1999, Le Roux 2012). The presence of a mixed assemblage of subtropical and cold-temperate plant species, such as *Nothofagus* (Bastos et al. 2013, Le Roux 2012), in Antarctica suggests sufficient soil development to support this vegetation. This, in turn, implies pre-weathering of the paleo-saprolite, whose location in the rock crevices preserved it from erosion. Further studies are necessary to better understand the characteristics of this paleo-saprolite and its connection to soil evolution in the Antarctic environment.

CONCLUSIONS

The northern sector of HP presented a wide variety of landscape features, and the general occurrence of ornithogenesis. Among the mapped landforms, the patterned ground occupied the largest area, while "Ornithogenic"/ Typical Gelorthents was the most dominant soil and the moss carpets was the predominant vegetation type. All soils of the rocky outcrops presented ornithogenic influence and varied between Gelisols, Entisols and Inceptsols. Soils of the cryoplanated platforms were mostly classified as Gelisols, whereas soils of the marine terraces were mainly Entisols.

The ornithogenic influence is the main contrasting factor of soils from the northern sector of HP, but vegetation cover, landforms, maritime climate and geology play an important role on conducing pedogenesis. Despite the intense current ornithogenic influence, soils of the marine terraces were the least developed, due to the youthfulness and lack of structure. Soils of the rocky outcrops were the most developed ones, even those closer to the glacier margin. This is justified due to the long-term phosphatization, and a pre-weathered saprolite between rock crevices, where moisture is high and the vegetation development greater, enhancing pedogenesis. The mineralogical composition of the clay fraction of these soils were predominantly composed by amorphous and crystalline phosphate minerals, as much as organo-metallic complexes. Soils of the platforms, represented mainly by the soils of patterned ground, presented a gradual pedogenetic development, conditioned by the influence of organisms and distance from the glacier, which indicates advanced periglacialism processes (mainly cryoturbation and cryoclasty).

Acknowledgments

This study was financed in part by the Coordenação de Aperfeiçoamento de Pessoal de Nível Superior - Brazil (CAPES) - Finance Code 001. We acknowledge the CAPES for concession the scholarship of the first author, and the Conselho Nacional de Desenvolvimento Científico e Tecnológico - Brazil (CNPq) for financial support of this project. This study was part of the first author's dissertation. This work is a contribution of Institute of Science and Technology of the Cryosphere - TERRANTAR group.

REFERENCES

ABAKUMOV E. 2018. Content of available forms of nitrogen, potassium and phosphorus in ornithogenic and other soils of the Fildes Peninsula (King George Island, Western Antarctica). Bio Comm 63: 109-116.

ABAKUMOV E, LUPACHEV A, ANDREEV M, WANG W & JI X. 2021a. The influence of brown and south polar skua on the content of plant nutrient in the soils from the Fildes Peninsula (King George Island, West Antarctica). Chem Ecol 37: 185-199.

ABAKUMOV EV, PARNIKOZA IYU, ZHIANSKI M, YANEVA R, LUPACHEV AV, ANDREEV MP, VLASOV DYU, RIANO J & JARAMILLO N. 2021b. Ornithogenic Factor of Soil Formation in Antarctica: A Review. Eurasian Soil Sci 54: 528-540.

ALMEIDA ICC, SCHAEFER CEGR, FERNANDES RBA, OLIVEIRA FS & PEREIRA TTC. 2021. Clay mineralogy and micropedology of phosphate-rich soils from Lions Rump, Maritime Antarctica. J South Am Earth Sci 105: 102967.

AMBROŽOVÁ K, HRBÁČEK F & LÁSKA K. 2020. The Summer Surface Energy Budget of the Ice-Free Area of Northern James Ross Island and Its Impact on the Ground Thermal Regime. Atmosphere (Basel) 11: 877.

ANDRADE AM DE, MICHEL RFM, BREMER UF, SCHAEFER CEGR & SIMÕES JC. 2018. Relationship between solar radiation and surface distribution of vegetation in Fildes Peninsula and Ardley Island, Maritime Antarctica. Int J Remote Sens 39: 2238-2254.

ARMIENTI P & BARONI C. 1999. Cenozoic climatic change in Antarctica recorded by volcanic activity and landscape evolution. Geology 27: 617-620.

ATCM XXXV. 2012. Management Plan for Antarctic Specially Protected Area No 161. Final Report of the Thirty-fifth Antarctic Treaty Consultative Meeting.

BALKS MR, LÓPEZ-MARTÍNEZ J, GORYACHKIN SV, MERGELOV NS, SCHAEFER CEGR, SIMAS FNB, ALMOND PC, CLARIDGE GGC, MCLEOD M & SCARROW J. 2013. Windows on Antarctic soil-landscape relationships: Comparison across selected regions of Antarctica. Geol Soc Spec Publ 381: 397-410.

BALLANTYNE CK. 2013. Paraglacial Geomorphology. Encyclopedia of Quaternary Science: Second Edition 21: 553-565.

BARSCH D & MÄUSBACHER R. 1986. New Data on the Relief Development of the South Shetland Islands, Antarctica. Interdiscip Sci Rev 11: 211-218.

BAS - BRITISH ANTARCTIC SURVEY. 2020. Antarctic Meteorology. https://legacy.bas.ac.uk/met/data.html.

BASTOS BL, DUTRA TL, WILBERGER TP & TREVISAN C. 2013. Uma flora do final do cretáceo na ilha nelson, ilhas Shetland do Sul, Península Antártica. Rev Bras de Paleontol 16: 441-464.

BLUME H-P, BEYER L, KALK E & KUHN D. 2002. Weathering and Soil Formation 154: 115-138.

BOCKHEIM JG. 2015. The Soils of Antarctica, Cham: Springer International Publishing, 11-49 p.

BOCKHEIM JG, LUPACHEV AV, BLUME HP, BÖLTER M, SIMAS FNB & MCLEOD M. 2015. Distribution of soil taxa in Antarctica: A preliminary analysis. Geoderma 245-246: 104-111.

BOCKHEIM JG & TARNOCAI C. 1998. Recognition of cryoturbation for classifying permafrost-affected soils. Geoderma 81: 281-293.

BOCKHEIM JG & UGOLINI FC. 1990. A Review of Pedogenic Zonation in Well-Drained Soils of the Southern Circumpolar Region. Quat Res 34: 47-66.

BOWMAN RA. 1989. A sequential extraction procedure with concentrated sulfuric acid and dilute base for soil organic phosphorus. Soil Sci Soc Am J 53: 362-366.

CAMPBELL IB & CLARIDGE GGC. 1987. Antarctica: Soils, weathering processes and environment, 1-368 p.

CASTRO MF, MEIER M, NEVES JCL, FRANCELINO MR, SCHAEFER CEGR & OLIVEIRA TS. 2022. Influence of different seabird species on trace metals content in Antarctic soils. An Acad Bras Cienc 94: e20210623.

CASTRO MF, NEVES JCL, FRANCELINO MR, SCHAEFER CEGR & OLIVEIRA TS. 2021. Seabirds enrich Antarctic soil with trace metals in organic fractions. Sci Total Environ 785: 147271.

CONVEY P & PECK LS. 2019. Antarctic environmental change and biological responses. Sci Adv 5.

DA SILVA TH, SILVA DAS, DE OLIVEIRA FS, SCHAEFER CEGR, ROSA CA & ROSA LH. 2020. Diversity, distribution, and ecology of viable fungi in permafrost and active layer of Maritime Antarctica. Extremophiles 24: 565-576.

DAHLGREN RA. 1994. Quantification of Allophane and Imogolite. In: AMONETTE JE & ZELAZNY LW (Eds), Quantitative Methods in Soil Mineralogy, Madison: Soil Science Society of America, p. 430-451.

DEL VALLE RA, MONTALTI D & INBAR M. 2002. Mid-Holocene macrofossil-bearing raised marine beaches at Potter Peninsula, King George Island, South Shetland Islands. Antarct Sci 14: 263-269.

DURÁN J, RODRÍGUEZ A, HEIÐMARSSON S, LEHMANN JRK, DEL MORAL Á, GARRIDO-BENAVENT I & DE LOS RÍOS A. 2021. Cryptogamic cover determines soil attributes and functioning in polar terrestrial ecosystems. Sci Total Environ 762: 143169.

FERRARI FR, SCHAEFER CEGR, PEREIRA AB, THOMAZINI A, SCHMITZ D & FRANCELINO MR. 2021. Coupled soil-vegetation changes along a topographic gradient on King George Island, maritime Antarctica. Catena (Amst) 198: 105038.

FERRARI FR, THOMAZINI A, PEREIRA AB, SPOKAS K & SCHAEFER CEGR. 2022. Potential greenhouse gases emissions by different plant communities in maritime Antarctica. An Acad Bras Cienc 94: e20210602.

FRANCELINO MR, SCHAEFER CEGR, SIMAS FNB, FILHO EIF, DE SOUZA JJLL & DA COSTA LM. 2011. Geomorphology and soils distribution under paraglacial conditions in an ice-free area of Admiralty Bay, King George Island, Antarctica. Catena (Amst) 85: 194-204.

GARRIDO-BENAVENT I, PÉREZ-ORTEGA S, DURÁN J, ASCASO C, POINTING SB, RODRÍGUEZ-CIELOS R, NAVARRO F & DE LOS RÍOS A. 2020. Differential Colonization and Succession of Microbial Communities in Rock and Soil Substrates on a Maritime Antarctic Glacier Forefield. Front Microbiol 11: 1-19.

GONZÁLEZ-GUZMÁN A, OLIVA M, SOUZA-JÚNIOR VS, PÉREZ-ALBERTI A, RUIZ-FERNÁNDEZ J & OTERO XL. 2017. Biota and geomorphic processes as key environmental factors controlling soil formation at Elephant Point, Maritime Antarctica. Geoderma 300: 32-43.

HALL BL. 2010. Holocene relative sea-level changes and ice fluctuations in the South Shetland Islands. Glob Planet Change 74: 15-26.

HALLET B. 2013. Stone circles: form and soil kinematics. Philos Trans Royal Soc 371: 20120357.

HAUS NW, WILHELM KR, BOCKHEIM JG, FOURNELLE J & MILLER M. 2016. A case for chemical weathering in soils of Hurd Peninsula, Livingston Island, South Shetland Islands, Antarctica. Geoderma 263: 185-194.

HJORT C, BJÖRCK S, INGÓLFSSON Ó & MÖLLER P. 1998. Holocene deglaciation and climate history of the northern Antarctic Peninsula region: A discussion of correlations between the Southern and Northern Hemispheres. Ann Glaciol 27: 110-112.

IUSS WORKING GROUP WRB. 2014. World reference base for soil resources 2014. International soil classification system for naming soils and creating legends for soil maps, 1-191 p.

JEONG GY & YOON HI. 2001. The origin of clay minerals in soils of King George Island, South Shetland Islands, West Antarctica, and its implications for the clay-mineral compositions of marine sediments. J Sediment Res 71: 833-842.

JOHN BS & SUGDEN DE. 1971. Raised marine features and phases of glaciation in the South Shetland Islands. BAS Bulletin 24: 45-111.

KJELDAHL C. 1883. A new method for the determination of nitrogen in organic matter. Z Anal Chem 22: 366-382.

LEE Y Il, LIM HS & YOON H Il. 2004. Geochemistry of soils of King George Island, South Shetland Islands, West Antarctica: Implications for pedogenesis in cold polar regions. Geochim Cosmochim Acta 68: 4319-4333.

LE ROUX JP. 2012. A review of Tertiary climate changes in southern South America and the Antarctic Peninsula. Part 2: Continental conditions. Sediment Geol 247-248: 21-38.

LONGTON RE. 1988. Biology of polar bryophytes and lichens, New York, NY: Cambridge University Press, 391 p.

LOPES DDV, OLIVEIRA FS DE, SOUZA JJLL De, MACHADO MDR & SCHAEFER CEGR. 2022. Soil pockets phosphatization and chemical weathering of sites affected by flying birds of Maritime Antarctica. An Acad Bras Cienc 94: e20210595.

LOPES D DO V, SCHAEFER CEGR, SOUZA JJLL DE, OLIVEIRA FS DE, SIMAS FNB, DAHER M & GJORUP DF. 2019. Concretionary horizons, unusual pedogenetic processes and features of sulfate affected soils from Antarctica. Geoderma 347: 13-24.

LOPES D DO V, SOUZA JJLL DE, SIMAS FNB, OLIVEIRA FS de & SCHAEFER CEGR. 2021. Hydrogeochemistry and chemical weathering in a periglacial environment of Maritime Antarctica. Catena (Amst) 197: 104959.

LÓPEZ-MARTÍNEZ J, SERRANO E, SCHMID T, MINK S & LINÉS C. 2012. Geomorphology Periglacial processes and landforms in the South Shetland Islands (northern Antarctic Peninsula region). Geomorphology 155-156: 62-79.

MACHADO M DE R, OLIVEIRA FS DE, SCHAEFER CEGR, FRANCELINO MR & MICHEL RFM. 2019. Paisagens polares não glaciais (proglacial, paraglacial e periglacial): revisão de conceitos e constribuições da pesquisa pedogeomorfológica brasileira. Rev Bras de Geomorfol 20: 603-622.

MCKEAGUE JA & DAY JH. 1966. DITHIONITE AND OXALATE EXTRACTABLE FE AND AI AS AIDS IN DIFFERENTIATING VARIOUS CLASSES OF SOILS. Can J Soil Sci 46: 13-22.

MEHRA OP & JACKSON ML. 1960. IRON OXIDE REMOVAL FROM SOILS AND CLAYS BY A DITHIONITE-CITRATE SYSTEM BUFFERED WITH SODIUM BICARBONATE. Clay and Clay Minerals 7: 317-327.

MENDONÇA T, MELO VF, SCHAEFER CEGR, SIMAS FNB & MICHEL RFM. 2013. Clay Mineralogy of Gelic Soils from the Fildes Peninsula, Maritime Antarctica. Soil Sci Soc Am J 77: 1842-1851.

MICHEL RFM, SCHAEFER CEGR, DIAS LE, NOGUEIRA F, SIMAS, BENITES VDM & MENDONÇA E DE S. 2006. Ornithogenic Gelisols (Cryosols) from Maritime Antarctica: Pedogenesis, Vegetation, and Carbon Studies. Soil Sci Soc Am J 70: 1370-1376.

MICHEL RFM, SCHAEFER CEGR, LÓPEZ-MARTÍNEZ J, SIMAS FNB, HAUS NW, SERRANO E & BOCKHEIM JG. 2014. Geomorphology Soils and landforms from Fildes Peninsula and Ardley Island, Maritime Antarctica. Geomorphology 225: 76-86.

MICHEL RFM, SCHAEFER CEGR, SIMAS FMB, FRANCELINO MR, FERNANDES-FILHO EI, LYRA GB & BOCKHEIM JG. 2014. Active-layer thermal monitoring on the Fildes Peninsula, King George Island, maritime Antarctica. Solid Earth 5: 1361-1374.

MOURA LZ, BIAS EDS & BRITES R. 2014. Evaluation of Digital Elevation Models (DEM) Vertical Accuracy in the Paranoá and São Bartolomeu River Basins. Rev Bras Cartogr 66: 1-14.

MYRCHA A, PIETR SJ & TATUR A. 1985. The Role of Pygoscelid Penguin Rookeries in Nutrient Cycles. In: SIEGFRIED WR et al. (Eds), Antarctic Nutrient Cycles and Food Webs, Springer-Verlag Berlin Heidelberg, p. 156-162.

NAVAS A, LÓPEZ-MARTÍNEZ J, CASAS J, MACHÍN J, DURÁN JJ, SERRANO E, CUCHI J-A & MINK S. 2008. Soil characteristics on varying lithological substrates in the South Shetland Islands, maritime Antarctica. Geoderma 144: 123-139.

OCHYRA R, LEWIS SMITH RI & BEDNAREK-OCHYRA H. 2008. The Illustrated Moss Flora of Antarctica, Cambridge: Cambridge University Press, 1-726 p.

OLECH M. 2004. Lichens of King George Island, Antarctica, Institute of Botany of the Jagiellonian University, 1-390 p.

OLIVA M & RUIZ-FERNÁNDEZ J. 2017. Geomorphological processes and frozen ground conditions in Elephant Point (Livingston Island, South Shetland Islands, Antarctica). Geomorphology 293: 368-379.

OTERO XL, DE LA PEÑA-LASTRA S, PÉREZ-ALBERTI A, FERREIRA TO & HUERTA-DIAZ MA. 2018. Seabird colonies as important global drivers in the nitrogen and phosphorus cycles. Nat Commun 9.

OTERO XL, FERNÁNDEZ S, DE PABLO HERNANDEZ MA, NIZOLI EC & QUESADA A. 2013. Plant communities as a key factor in biogeochemical processes involving micronutrients (Fe, Mn, Co, and Cu) in Antarctic soils (Byers Peninsula, maritime Antarctica). Geoderma 195-196: 145-154.

PALLÀS R, VILAPLANA JM & SÀBAT F. 1995. Geomorphological and neotectonic features of Hurd Peninsula, Livingston Island, South Shetland Islands. Antarct Sci 7: 395-406.

PEREIRA TTC, SCHAEFER CEGR, KER JC, ALMEIDA CC, ALMEIDA ICC & PEREIRA AÔB. 2013. Genesis, mineralogy and ecological significance of ornithogenic soils from a semi-desert polar landscape at Hope Bay, Antarctic Peninsula. Geoderma 209-210: 98-109.

PIETR SJ, TATUR A & MYRCHA A. 1983. Mineralization of penguin excrements in the Admiralty Bay region (King George Island, South Shetland Islands, Antarctica). Polish Polar Resear 4: 97-112.

POELKING EL, SCHAEFER CER, FERNANDES FILHO EI, DE ANDRADE AM & SPIELMANN AA. 2015. Soil-landform-plant-community relationships of a periglacial landscape on Potter Peninsula, maritime Antarctica. Solid Earth 6: 583-594.

PRIETZEL J, PRATER I, COLOCHO HURTARTE LC, HRBÁČEK F, KLYSUBUN W & MUELLER CW. 2019. Site conditions and vegetation determine phosphorus and sulfur speciation in soils of Antarctica. Geochim Cosmochim Acta 246: 339-362.

PUDEŁKO R, ANGIEL P, POTOCKI M, JĘDREJEK A & KOZAK M. 2018. Fluctuation of Glacial Retreat Rates in the Eastern Part of Warszawa Icefield, King George Island, Antarctica, 1979-2018. Remote Sens (Basel) 10: 892.

PUTZKE J & PEREIRA AB. 2001. The Antarctic mosses with sepecial reference to the South Shetland Islands, 1 ed., Canoas: ULBRA, 196 p.

RAMÍREZ-FERNÁNDEZ L, TREFAULT N, CARÚ M & ORLANDO J. 2019. Seabird and pinniped shape soil bacterial communities of their settlements in Cape Shirreff, Antarctica. PLoS ONE 14: e0209887.

RODRIGUES WF, DE OLIVEIRA FS, SCHAEFER CEGR, GAUZZI T & LEITE MGP. 2021a. Geochemistry of Antarctic periglacial soils from Harmony Point, Nelson Island. Environ Earth Sci 80: 430.

RODRIGUES WF, DE OLIVEIRA FS, SCHAEFER CEGR, LEITE MGP & PAVINATO PS. 2021b. Phosphatization under birds' activity: Ornithogenesis at different scales on Antarctic Soilscapes. Geoderma 391: 114950.

RODRIGUES WF, OLIVEIRA FS, SCHAEFER CEGR, LEITE MGP, GAUZZI T, BOCKHEIM JG & PUTZKE J. 2019. Soil-landscape interplays at Harmony Point, Nelson Island, Maritime Antarctica: Chemistry, mineralogy and classification. Geomorphology 336: 77-94.

SCHAEFER CEGR, PEREIRA TTC, ALMEIDA ICC, MICHEL RFM, CORRÊA GR, FIGUEIREDO LPS & KER JC. 2017. Penguin activity modify the thermal regime of active layer in Antarctica: A case study from Hope Bay. Catena (Amst) 149: 582-591.

SCHAEFER CEGR, SIMAS FNB, GILKES RJ, MATHISON C, DA COSTA LM & ALBUQUERQUE MA. 2008. Micromorphology and microchemistry of selected Cryosols from maritime Antarctica. Geoderma 144: 104-115.

SCHMITZ D, SCHAEFER CERG, PUTZKE J, FRANCELINO MR, FERRARI FR, CORRÊA GR & VILLA PM. 2020b. How does the pedoenvironmental gradient shape non-vascular species assemblages and community structures in Maritime Antarctica? Ecol Indic 108: 105726.

SCHMITZ D, VILLA PM, MICHEL RFM, PUTZKE J, PEREIRA AB & SCHAEFER CEGR. 2022. Species composition, diversity and coverage pattern of associated communities of mosses-lichens along a pedoenvironmental gradient in Maritime Antarctica. An Acad Bras Cienc 94: e20200094.

SCHMITZ D, VILLA PM, PUTZKE J, MICHEL RFM, CAMPOS PV, NETO JAAM & SCHAEFER CEGR. 2020a. Diversity and species associations in cryptogam communities along a pedoenvironmental gradient on Elephant Island, Maritime Antarctica. Folia Geobot 55: 211-224.

SIMMS AR, DEWITT R, KOUREMENOS P & DREWRY AM. 2011. A new approach to reconstructing sea levels in Antarctica using optically stimulated luminescence of cobble surfaces. Quat Geochronol 6: 50-60.

SIMAS FNB, ERNESTO C, SCHAEFER GR, MELO VF, ALBUQUERQUE-FILHO MR, MICHEL RFM, PEREIRA VV, GOMES MRM & LIOVANDO M. 2007. Ornithogenic cryosols from Maritime Antarctica: Phosphatization as a soil forming process. Geoderma 138: 191-203.

SIMAS FNB, SCHAEFER CEGR, FILHO MRA, FRANCELINO MR, FILHO EIF & DA COSTA LM. 2008. Genesis, properties and classification of Cryosols from Admiralty Bay, maritime Antarctica. Geoderma 144: 116-122.

SIMAS FNB, SCHAEFER CEGR, MELO VF, GUERRA MBB, SAUNDERS M & GILKES RJ. 2006. Clay-sized minerals in permafrost-affected soils (Cryosols) from King George Island, Antarctica. Clays Clay Miner 54: 721-736.

SIMAS FNB, SCHAEFER CEGR, MICHEL RFM, FRANCELINO MR & BOCKHEIM JG. 2015. Soils of the South Orkney and South Shetland Islands, Antarctica. In: Bockheim JG, editor. Springer, p. 227-273.

SIQUEIRA RG, LOPES DV, SOUZA JJLL DE, SCHAEFER CEGR, SOUZA CD, OLIVEIRA FS DE & FERNANDES FILHO EI. 2022. Acid sulfate soils from Antarctica: genesis and properties along a climatic gradient. An Acad Bras Cienc 94: e20210625.

SLAYMAKER O. 2011. Criteria to distinguish between periglacial, proglacial and paraglacial environments. Quaest Geogr 30: 85-94.

SMELLIE JL, PANKHURST RJ, THOMSON MRA & DAVIES RES. 1984. The geology of the South Shetland Islands: VI. Stratigraphy, geochemistry and evolution, Cambridge: Cambridge, 85 p.

SSS. 1999. Soil Taxonomy: A basic system of Soil Classification for Making and Interpreting Soil Surveys, 2 ed., United States Department of Agriculture, 886 p.

SSS. 2014. Keys to Soil Taxonomy, 12 ed., United States Department of Agriculture, 360 p.

TATUR A. 1989. Ornithogenic soils of the maritime Antarctic. Pol Polar Res 10: 481-532.

TATUR A. 2002. Ornithogenic Ecosystems in the Maritime Antarctic — Formation, Development and Disintegration. In: BEYER L & BÖLTER M (Eds), Geoecology of Antarctic Ice-Free Coastal Landscapes, Berlin: Springer, p. 161-184.

TATUR A & BARCZUK A. 1985. Ornithogenic Phosphates on King George Island in the Maritime Antarctic. In: SIEGFRIED WR et al. (Eds), Antarctic Nutrient Cycles and Food Webs, Springer-Verlag Berlin Heidelberg, p. 163-168.

TATUR A & KECK A. 1990. Phosphates in ornithogenic soils of the maritime Antarctica. In: Proc. NIPR Symp. Polar Biol, p. 133-150.

TATUR A & MYRCHA A. 1984. Ornithogenic soils on King George lsland, South Shetland lslands (Maritime Antarctic Zone). Pol Polar Res 5: 31-60.

TATUR A, MYRCHA A & NIEGODZISZ J. 1997. Formation of abandoned penguin rookery ecosystems in the maritime Antarctic. Polar Biol 17: 405-417.

TEIXEIRA PC, DONAGEMMA GK, FONTANA A & TEIXEIRA WG. 2017. Manual de métodos de análise de solo, 3 ed., Brasília: Embrapa, 1-699 p.

TUCKER CJ. 1978. Red and Photographic Infrared Linear Combinations for Monitoring Vegetation.

TURNER J & PENDLEBURY S. 2004. The international Antarctic weather forecasting handbook, Cambridge: British Antarctic Survey, 1-685 p.

YEOMANS JC & BREMNER JM. 1988. A rapid and precise method for routine determination of organic carbon in soil. Commun Soil Sci Plant Anal 19: 1467-1476.

ZHU R, LIU Y, MA E, SUN J, XU H & SUN L. 2009. Greenhouse gas emissions from penguin guanos and ornithogenic soils in coastal Antarctica: Effects of freezing – thawing cycles. Atmos Environ 43: 2336-2347.

ZHU R, SUN J, LIU Y, GONG Z & SUN L. 2011. Potential ammonia emissions from penguin guano, ornithogenic soils and seal colony soils in coastal Antarctica: effects of freezing-thawing cycles and selected environmental variables. Antarct Sci 23: 78-92.

How to cite

SACRAMENTO IF, SCHAEFER CEGR, SIQUEIRA RG, CORRÊA GR, PUTZKE J, MICHEL RFM & FRANCELINO MR. 2023. Ornithogenesis and soil-landscape interplays at northern Harmony Point, Nelson Island, Maritime Antarctica. An Acad Bras Cienc 95: e20230722. DOI 10.1590/0001-3765202320230722.

Manuscript received on June 28, 2022;
accepted for publication on November 16, 2023

IORRANA F. SACRAMENTO[1]
https://orcid.org/0000-0002-9440-0034

CARLOS ERNESTO G.R. SCHAEFER[1]
https://orcid.org/0000-0001-7060-1598

RAFAEL G. SIQUEIRA[1]
https://orcid.org/0000-0003-2779-136X

GUILHERME R. CORRÊA[2]
https://orcid.org/0000-0001-8763-7204

JAIR PUTZKE[3]
https://orcid.org/0000-0002-9018-9024

ROBERTO F.M. MICHEL[4]
https://orcid.org/0000-0001-5951-4610

MÁRCIO R. FRANCELINO[1]
https://orcid.org/0000-0001-8837-1372

[1]Universidade Federal de Viçosa, Departamento de Solos, Av. Peter Henry Rolfs, s/n, Campus Universitário, 36570-900 Viçosa, MG, Brazil

[2]Instituto de Geografia, Av. João Naves de Ávila, 2121, Campus Santa Mônica, Bloco 1H, Sala 25, Santa Mônica, 38400-902 Uberlândia, MG, Brazil

[3]Programa de Pós-Graduação em Ciências Biológicas, Universidade Federal do Pampa, Av. Antônio Trilha, Campus de São Gabriel, Centro, 97300-000 São Gabriel, RS, Brazil

[4]Universidade Estadual de Santa Cruz, Departamento de Ciências Agrárias e Ambientais, Rodovia Jorge Amado, Km 1, 45662-900 Ilhéus, BA Brazil

Correspondence to: **Iorrana Figueiredo Sacramento**
E-mail: iorranafigueiredos@gmail.com

Author contributions

Iorrana F. Sacramento: conceptualization, formal analysis, investigation, methodology, visualization, writing, review, and editing. Carlos Ernesto G.R. Schaefer: funding acquisition, conceptualization, investigation, methodology, writing, review, and editing. Rafael G. Siqueira: investigation, visualization, writing, review, and editing. Guilherme R. Corrêa, Jair Putzke and Roberto F. M. Michel: conceptualization, methodology, review, and editing. Márcio R. Francelino: funding acquisition, conceptualization, review, and editing.